Journal of Archaeological Science 105 (2019) 97–115

Contents lists available at ScienceDirect

Journal of Archaeological Science

journal homepage: www.elsevier.com/locate/jas

The beginning of faience in China: A review and new evidence

Yi-Xian Lin[a,*], Thilo Rehren[b,c], Hui Wang[d], Xiao-Yan Ren[e], Jian Ma[f]

[a] College of Applied Arts and Science of Beijing Union University, 197 Bei Tu Cheng Xi Road, Beijing, 100191, PR China
[b] UCL Institute of Archaeology, London, WC1H 0PY, UK
[c] The Cyprus Institute, Science and Technology in Archaeology and Culture, 2121, Nicosia, Cyprus
[d] Gansu Provincial Institute of Archaeology and Cultural Relics, 165 Heping Road, Lanzhou, Gansu, 730000, PR China
[e] Qinghai Provincial Institute of Archaeology and Cultural Relics, 15 Weimin Lane, Xining, Qinghai, 810000, PR China
[f] School of Cultural Heritage, Northwest University, 229 Taibai Beilu, Xi'an, Shaanxi, 710069, PR China

ARTICLE INFO

Keywords:
Faience
China
Zhou

ABSTRACT

Despite decades of research into faience artefacts in China, many questions remain about how, where and by whom this technology began. This study combines published and new results of chemical analysis, morphology and chronology of the earliest faience beads uncovered from Xinjiang, Qinghai, Gansu, Shaanxi and Shanxi to suggest that at the latest in the mid-second millennium BC faience was first imported from the northern Caucasus or the Steppe into Xinjiang. In the second half of the second millennium, the Kayue people in Qinghai began making high potash faience, before the Zhou people in Shaanxi and Shanxi learnt and distributed the technology more widely across central China, probably via contacts with their pastoralist neighbours.

1. Introduction

Finds of early faience in the core area of China are relatively rare, appearing suddenly in the Central Plains along with the rise of the Western Zhou dynasty (1040s-771 BC; Hommel and Sax, 2014). Due to this apparent link and the significance of the Western Zhou for the development of Chinese society, questions of its beginning, e.g. its location, timing and origin, continue to receive strong interest. For about a millennium faience was used across a wide area, mostly in form of beads or pendants in burial contexts, only to disappear during the Han dynasty (202 BC-AD 220) or soon after (Ma et al., 2009). Since the 1980s, interest in this material arose from excavations in Yu Kingdom tombs and Beilu graves of the Western Zhou, Shaanxi province, where thousands of faience beads or fragments were uncovered. These beads were worn by ordinary people which led to them being interpreted as local production (Wang, 1991).

Various scientific techniques have been applied to study these early faience objects (e.g. Zhang et al., 1983; Brill et al., 1991; Fu and Gan, 2006; Zhang and Ma, 2009; Hao et al., 2014; Gu et al., 2014; Lei and Xia, 2015) and identified different compositional types based on their soda to potash ratio. Received discussion holds that faience glazed using soda-rich plant ash is likely to originate in Egypt or the Middle East (Tite et al., 2006; Vandiver, 2008: 38–41; Bouquillon et al., 2008: 93–97). In contrast, potash-dominated faience is thought to be of genuine Chinese origin, although no specific production regions have been proposed to date (Fu and Gan, 2006). This thinking has been later expanded to argue that soda-rich faience was made somewhere on the route from Egypt to central China during the early Western Zhou period, while potash-rich faience was thought to have been locally made during the middle to late Western Zhou (Lei and Xia, 2015). Recently, 13 faience beads from the Ya'er cemetery in eastern Xinjiang, dated broadly to 1050–300 BC, were investigated with computer tomography (CT) and energy dispersive X-ray fluorescence (ED-XRF), and a possible 'faience road' from western Asia through Xinjiang to central China was suggested (Liu et al., 2017).

Most of the previous studies are based on non-destructive surface analyses, and the total concentrations of alkalis measured are either very low or even almost completely absent due to severe weathering; therefore, it is hard to verify the current conclusions based on these analyses. Furthermore, since nearly all cemeteries from which early faience objects were uncovered were used over many centuries, a more precise dating for each sample is seldom available, which impedes further interpretation.

With the benefit of access to unpublished excavation materials, the first author conducted a comprehensive survey of vitreous materials from Northwest China, including some faience beads that were not known before. We now aim to contribute to the debate on the origins of Chinese faience manufacture by adding new evidence of faience use within this region and extending the available compositional and microstructural data.

* Corresponding author.
E-mail address: yixian@buu.edu.cn (Y.-X. Lin).

https://doi.org/10.1016/j.jas.2019.03.007
Received 18 August 2018; Received in revised form 10 March 2019; Accepted 25 March 2019

Table 1
Provenance and description of faience finds that are no later than middle Western Zhou (950–850 BC).

Location of Sites	Date	Typology	Source
The Northwest Caspian Sea Region, the North Caucasus and adjacent steppe areas	Between the 4th and early 2nd millennium BC	ABDEFHIJKL	Shortland et al. (2007)
Saensayi, Xinjiang	17th - 15th cent. BC	K (and probably H)	Xinjiang Institute of Cultural Relics and Archaeology (2013): 63–65, PLATE 37.4
Tianshanbeilu, Xinjiang	1500–1400 BC	HK	Unpublished
Ya'er, Xinjiang	1050–910 BC	AH	Liu et al. (2017)
Shangsunjiazhai, Qinghai (Kayue)	1600/1300–1000 BC	AH	Unpublished
Banzhuwa, Qinghai	Middle to late phase of 1000–700 BC	HI	Unpublished
Tianma-Qucun, Shanxi	Late phase of Early to middle Western Zhou (1020–850 BC)	AH	Lei and Xia (2015)
Hengshui, Shanxi	Middle Western Zhou (950–850 BC)	ABHI	Archaeology Institute of Shanxi Province (2006): Fig. 19 and 23; Lei and Xia (2015)
Dahekou, Shanxi	Middle Western Zhou (950–850 BC)	AHI	Unpublished
Zhangjiapo, Shaanxi	Early to Middle Western Zhou (1040s-950 BC)	AB (and probably a slit ring-Jue and a few vessel fragments)	Institute of Archaeology Chinese, Academy of Social Sciences (1999): 53–54, 307–308, APPENDIX 8, PLATE 171.1& 172.2
Beilu, Shaanxi	Early to Middle Western Zhou (1040s-950 BC)	A	Luo (1995): 129, PLATE57.2 & 58.5
Zhuyuangou & Rujiazhuang, Shaanxi	Early phase of Middle Western Zhou (King Mu: 956–918 BC)	AHMN	Lu and Hu (1998): 239–242, 246, 268–269, 329–330, 379–381, 386, PLATE 25.1–3, 138.1–3, 177.1, 206.2–3
Liutaizi, Shandong	Late phase of Early Western Zhou (King Zhao: 977/75–957 BC)	H	Shandong Provincial Institute of Cultural Relics and Archaeology (1996); Shandong Provincial Institute of Cultural Relics and Archaeology et al., (2010): 184.
Yujiawan, Gansu	Middle Western Zhou (950–850 BC)	A	Institute of Cultural Relics and Archaeology of Gansu Province (2009): PLATE 11.5
Pingdingshan, Henan	Middle Western Zhou (950–850 BC)	A	Gan et al. (2009)

A) Spherical/ellipsoidal; B) Small bi-conical; C) Small bi-conical with protrusions; D) Disk; E) Short cylindrical; F) Short cylindrical with horns or warts; G) Standard cylindrical; H) Smooth tube; I) Tube with protrusions; J) Tube with relief ornamentation; K) Segmented tube; L) Segmented tube with protrusions; M) Big bi-conical; N) Big bi-conical with protrusions.

2. Materials and archaeological backgrounds

In order to test the hypothesis that local manufacture of faience in northern China began from the middle Western Zhou, based on foreign influence, we base this study on faience excavated in China that can be securely dated to no later than the middle of Western Zhou (Table 1). The major sites are all cemeteries in Xinjiang, eastern Qinghai, eastern Gansu and the Jin-Shan area (that is, Shanxi and Shaanxi) (Fig. 1).

2.1. Xinjiang

The earliest known faience in China so far was a string of segmented beads uncovered from Saensayi cemetery, Xinjiang, which can be dated by pottery typology to the 17th to 15th century BC (Fig. 2a; Xinjiang Institute of Cultural Relics and Archaeology, 2013: 63–65, PLATE 37.4). Some tubes or short cylindrical beads of the same time span (Xinjiang Institute of Cultural Relics and Archaeology, 2013: 65–66, 82–84, PLATE 39.4 & 52.5) were probably also made from faience, but their material identification remains uncertain. Interestingly, segmented faience beads buried during the same period or a little bit later were identified also from the Tianshanbeilu cemetery, the earliest Bronze Age site in eastern Xinjiang (Li, S., 2002). Among a total of 5460 beads, mostly made of talc or turquoise, four faience beads and tubes survive in a single burial (M200, Fig. 2b). The pottery from M200 closely matches that from M683 which is dated by ^{14}C to about 3200 ± 30 BP (IVPPXJ-0039 M683, human bone sample) and 1525-1420 cal BC at 95.4% (IntCal 13), therefore M200 can most likely be attributed to 1500–1400 BC. Faience did not appear again in this area until some hundred years later in the nearby Ya'er cemetery (Liu et al., 2017).

2.2. Qinghai

In the vast area between Xinjiang and the Zhou cultural sphere, only the faience from the Kayue culture in Qinghai can be likely dated to no later than the middle of Western Zhou. In the very large cemetery at Shangsunjiazhai, consisting of 1,112 Neolithic to Bronze Age burials (Ren, 2013: 69–83), nine tombs of Kayue culture and two of 'Tangwang type' were identified to contain a few to some tens of faience beads (Li Zhi-Xin, pers. Com.; Fig. 3 a-b). They are mostly spherical or ellipsoidal beads and tubes. Seven burials of the 'Tangwang type' cut into Kayue burials, revealing a stratigraphic sequence (Xu, 1988, 1989). Five tombs of the 'Tangwang type' have available ^{14}C dates (Institute of Archaeology, Chinese Academy of Social Sciences, 1991: 287–288) (Appendix A). Since the dated tombs M333 and M989 represent the early and late phases of the 'Tangwang type' (Xu, 1989), an approximate date of the 'Tangwang type' can be inferred as from Western Zhou (Yu, 1985: 203) to Eastern Zhou (Shui, 2001: 243), or 1000 to 400 BC. The painted pottery of the earliest phase of the Kayue culture in Shangsunjiazhai is outstandingly reminiscent of that of the late Qijia culture (Xu, 1988, 1989), placing the upper limitation of the Kayue culture in this cemetery roughly around 1600 BC (Yu, 1985: 203; Miyake, 2005). But burials of the early phase are relatively few, therefore, the majority of the Kayue culture in Shangsunjiazhai can be attributed to the middle to late phase of this culture, or tentatively dates from c. 1600/1300 BC (Miyake, 2005) to c. 1000 BC.

2.3. Zhou realm

The earliest faience discoveries within the Zhou realm were mainly concentrated in two areas: the Plain of Zhou (Zhouyuan), settled by the

Fig. 1. Map showing the location of key sites in the text (modified based on the standard map issued by the Ministry of Natural Resources of China).

ancestors of the royal Zhou, and Qucun, the Jin political centre. Some sporadic faience beads were also found in the Zhou lineage at Yujiawan (Gansu), the Guo lineage at Shangcunling in Sanmenxia (Henan) and the Pang lineage at Liutaizi (Shandong). They are roughly dated from the 1040s to 950 BC, contemporary with the finds in Ya'er, Xinjiang. Spherical or ellipsoidal (Fig. 3 c-d) types and tubes were common, with some new shapes such as bi-conical, tube and big bi-conical with protrusions occurring, too (Fig. 4 a-b).

Among the limited faience finds in the Zhou cultural sphere during this period that have been properly analysed, two beads from the tomb M113 of Tianma-Qucun are probably the earliest. They are securely dated to the late phase of early Western Zhou (King Zhao, 977/75–957 BC) by typological evaluation of "diagnostic" objects, or to 1020–930 BC by ^{14}C dating of a human bone sample (The School of Archaeology and Museology Beijing University & The Institute of Archaeology of Shanxi Province, 2001; Li, B., 2002). As Lei and Xia (2015) reported,

Fig. 2. Faience beads from Bronze Age Xinjiang: a) Saensayi; b) Tianshanbeilu.

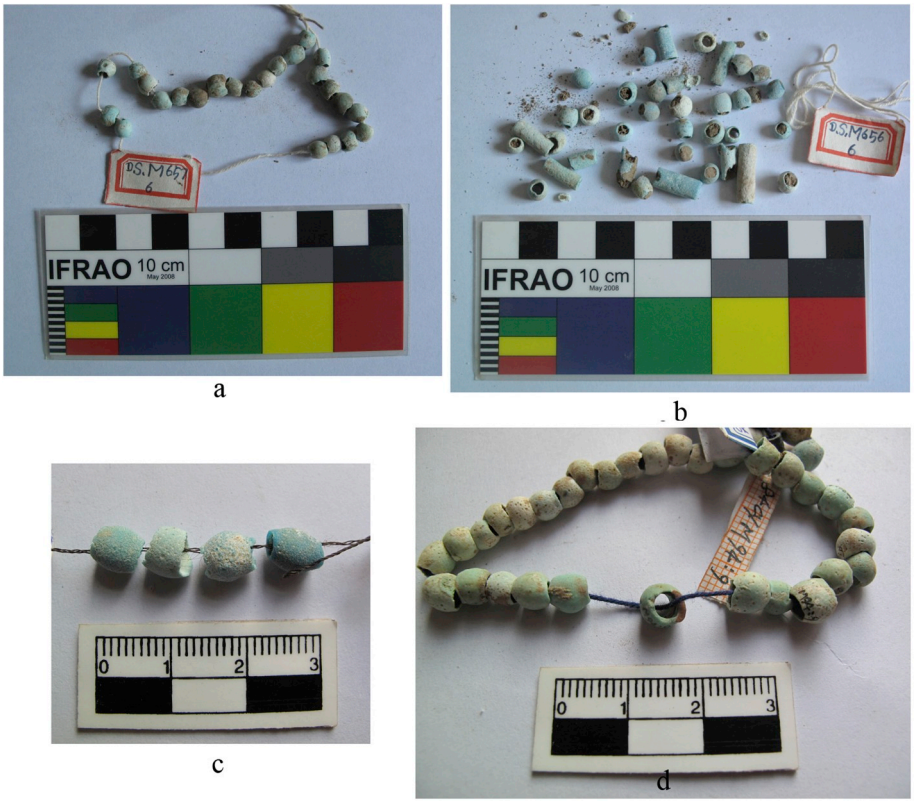

Fig. 3. Faience beads from Qinghai and Gansu: a) M657 of Kayue culture at Shangsunjiazhai; b) M656 of Kayue culture at Shangsunjiazhai; c) M19 at Yujiawan; d) M94 at Yujiawan.

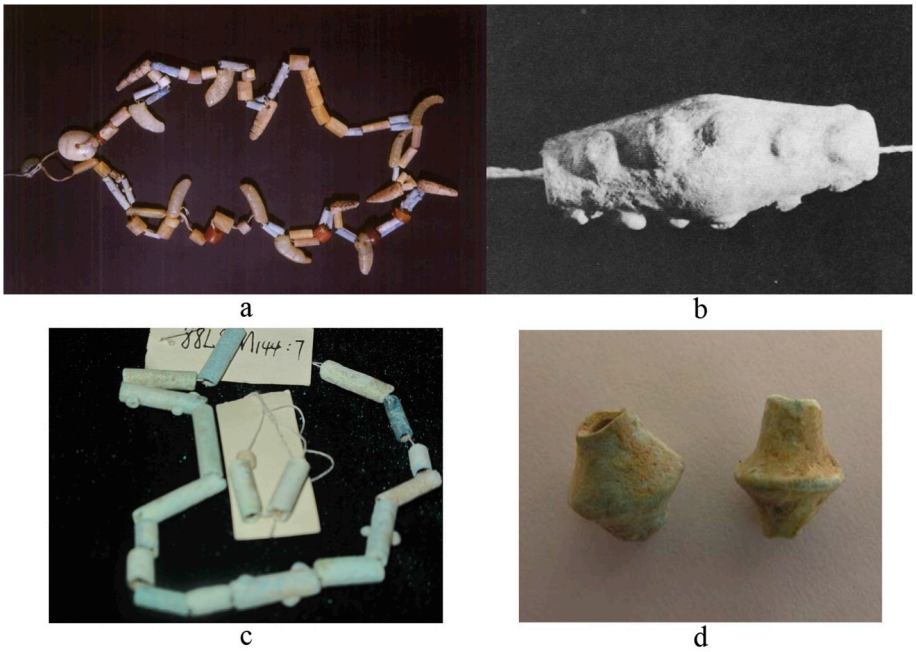

Fig. 4. Faience beads from Qinghai and Jin-Shan showing some common characters: a) M216 at Zhangjiapo (after Institute of Archaeology, Chinese Academy of Social Sciences, 1999); b) from Yu Kingdom cemetery (after Wang, 1991); c) M144 at Banzhuwa; d) from Yangqu.

they are soda-enriched in composition, thus leading the scholars to believe that they were either from Egypt or regions influenced by Egyptian technology. Similarly, three beads from M94 at Yujiawan of the middle Western Zhou (Institute of Cultural Relics and Archaeology of Gansu Province, 2009: 124–141) were also reported to have soda-rich plant ash compositions and thought to be influenced from Egypt or Western Asia (Zhang and Ma, 2009). Some other beads from Tianma-Qucun, Hengshui, Zhuyuangou, etc. of middle Western Zhou contexts were all rich in potassium (Lei and Xia, 2015).

Table 2
Faience beads analysed in this paper.

Code	Site	Burial	Date	Culture	Morphology	Analytical methods
TB1-1 to −6 TB2-1, −2	Tianshanbeilu, Xinjiang	M200	1500–1400 BC	Siba	Tubular & segmented	SEM-EDS
TB3, 4					Segmented	
QDS7A	Shangsunjiazhai, Qinghai	M554	1600/1300–1000 BC	Kayue	Round	
QDS10-1		M504				
QDS11-1, −2		M756				
QDS9A		M601	1000–400 BC	'Tangwang type'	Tubular	
84CYM19–1:1	Yujiawan, Gansu	M19	Middle Western Zhou (950–850 BC)	Zhou lineage	Round	SEM-EDS & LA-ICP-MS
84CYM19–1:3						
84CYM19–1:4						
CYM 1-4		M94				LA-ICP-MS
SYD1A	Dahekou, Shanxi	M2	Middle Western Zhou (950–850 BC)	Probably *Di* people	Tubular	SEM-EDS
SYD3A		M5001			Round	
SJH3	Tianma-Qucun, Shanxi	M113	Early to Middle Western Zhou (1040s–950 BC)	Jin lineage	Tubular	

2.4. Typological analysis

The above faience finds can be divided into three stages by chronology as follows: 1) 1700 BC to 1500/1400 BC, Saensayi and Tianshanbeilu, Xinjiang; 2) 1600/1300 BC to 1000 BC, Shangsunjiazhai (Kayue), Qinghai; 3) 1040s BC to 950/910 BC, Jin-Shan area and its vicinity as well as Ya'er in Xinjiang. Typologically, segmented tubes and tubes with protrusions are of particular interest. As Shortland et al. (2007) indicated, they first appeared in the northern Caucasus and were made for a long time and from various materials, indicating a local origin. Furthermore, Rawson (2013: 63) proposed that the tubular form with protrusions could not have been independently invented in China. The typological comparison (Table 1) shows that segmented tubes are restricted to stage 1 in Xinjiang, while tubes with protrusions first occurred at Hengshui in Jin-Shan at stage 3 and never appeared in Xinjiang. Provided that these morphologies were indeed diagnostic of foreign influence or stimulus, they could not have been introduced into the territory of present China at the same time. Therefore, the aforementioned hypothesis of a faience road from the outside via Xinjiang to Central China (Liu et al., 2017) deserves a careful re-investigation.

The bi-conical shape was thought to be associated with Chinese locally made potash-enriched faience during the middle Western Zhou (Lei and Xia, 2015). This type of faience beads has been excavated from the tomb M200 at Zhangjiapo in an early to middle Western Zhou context (Institute of Archaeology, Chinese Academy of Social Sciences, 1999: 308). In Zhangjiapo, tomb M163 from the middle Western Zhou yielded some faience vessel fragments and a slit ring-Jue that were quintessential for the Central Plain (Institute of Archaeology Chinese, Academy of Social Sciences, 1999: 307; Lu Lian-Cheng, pers. com.), implying an already quite mature faience making during the middle Western Zhou.

Another issue we may need to test is whether or not there was a potential interaction between Qinghai and Jin-Shan. Visually, beads from Qinghai and Jin-Shan show more similarities with each other than both with those from Xinjiang. From middle to late Western Zhou, faience tubes with protrusions were common in Jin-Shan. A special type of rhombic beads with bumps was excavated from the middle Western Zhou tomb BRM1 at Rujiazhuang (Wang, 1991; Lu and Hu, 1998: 329, 412), indicating a local adoption of foreign models. A string of tubular faience beads with protrusions was uncovered from a tomb of late Kayue culture at Banzhuwa, Hualong County, Qinghai (Fig. 4c; Qinghai Provincial Institute of Cultural Relics and ArchaeologyDepartment of History and Archaeology of Xibei University & Institute of Hualong County Culture Administration, 1996) that could be roughly dated to the middle to late phase of 1000 to 700 BC (Miyake, 2005), that is to say, later than their debut in Jin-Shan. Meanwhile, two bi-conical faience beads were identified during a survey on Yangqu, Qinghai of Kayue Culture (Fig. 4d, unpublished). Although there is no way to date Yangqu to any specific period of Kayue, and thus no reasonable comparison can be made with those popular bi-conical faience beads in Jin-Shan area, they do add more evidence of the similarity shared by these two areas.

2.5. Sampling

To address the above questions, samples from sites in Xinjiang, Qinghai, Gansu and Jin-Shan were studied. From Xinjiang, Gansu and Jin-Shan, we analysed relatively well-dated beads from Tianshanbeilu, Yujiawan (Fig. 3 c-d) and the Ba state cemetery of probable *Di* people at Dahekou, dating to the middle Western Zhou (Institute of Cultural Relics and Archaeology of Gansu Province, 2009: 124–130, 145–146; Joint Archaeological Team of Shanxi Provincial Institute of Archaeology, 2012; Xie Yao-Ting, pers. com.). In Qinghai, only samples from Shangsunjiazhai are suitable for our study, even though their dating is not quite precise (see above).

Tianshanbeilu (Xinjiang, sample code TB …). The 13 analysed faience fragments come from one broken segmented bead and 11 fragments collected from the store bag containing a further three beads. By visual observation, apart from the broken bead, the other three ones are all more or less worn and broken, so these fragments could belong to either of them. Ten samples had glass phases visible under SEM. To describe the glass, we follow the terminology established by Vandiver (2008), distinguishing between glass in the Interaction Layer (IAL) between the glaze and the body, and Inter-Particle Glass (IPG-BDY) found in the body of the beads, while for samples where it was difficult to clearly identify the relative location of the interstitial glass we use IPG. The 10 Tianshanbeilu samples showed either IAL (2), or IPG (3), or both (5).

Shangsunjiazhai (Qinghai, sample code QDS …). Seven beads from five tombs were sampled but one of them lacked a glass phase, while another seemed to be too weathered to produce proper information. The available five analyses come from five beads of four tombs; in all of them was sufficient IPG remaining for our analyses.

Yujiawan (Gansu, sample code CYM …). Four and three complete beads from tombs M94 and M19 respectively were analysed by LA-ICP-MS. Then the three beads from M19 were prepared for SEM-EDS analysis and reported here as three samples, each with IAL and IPG.

Dahekou (Shanxi, sample code SYD …). The available two analyses come from two beads from two tombs; in both, IPG was preserved.

Finally, another bead from tomb M113 from *Tianma-Qucun (Shanxi, sample code SJH)* was included in our analysis, in addition to the two already published (Lei and Xia, 2015). In total 25 samples from five sites were analysed (Table 2).

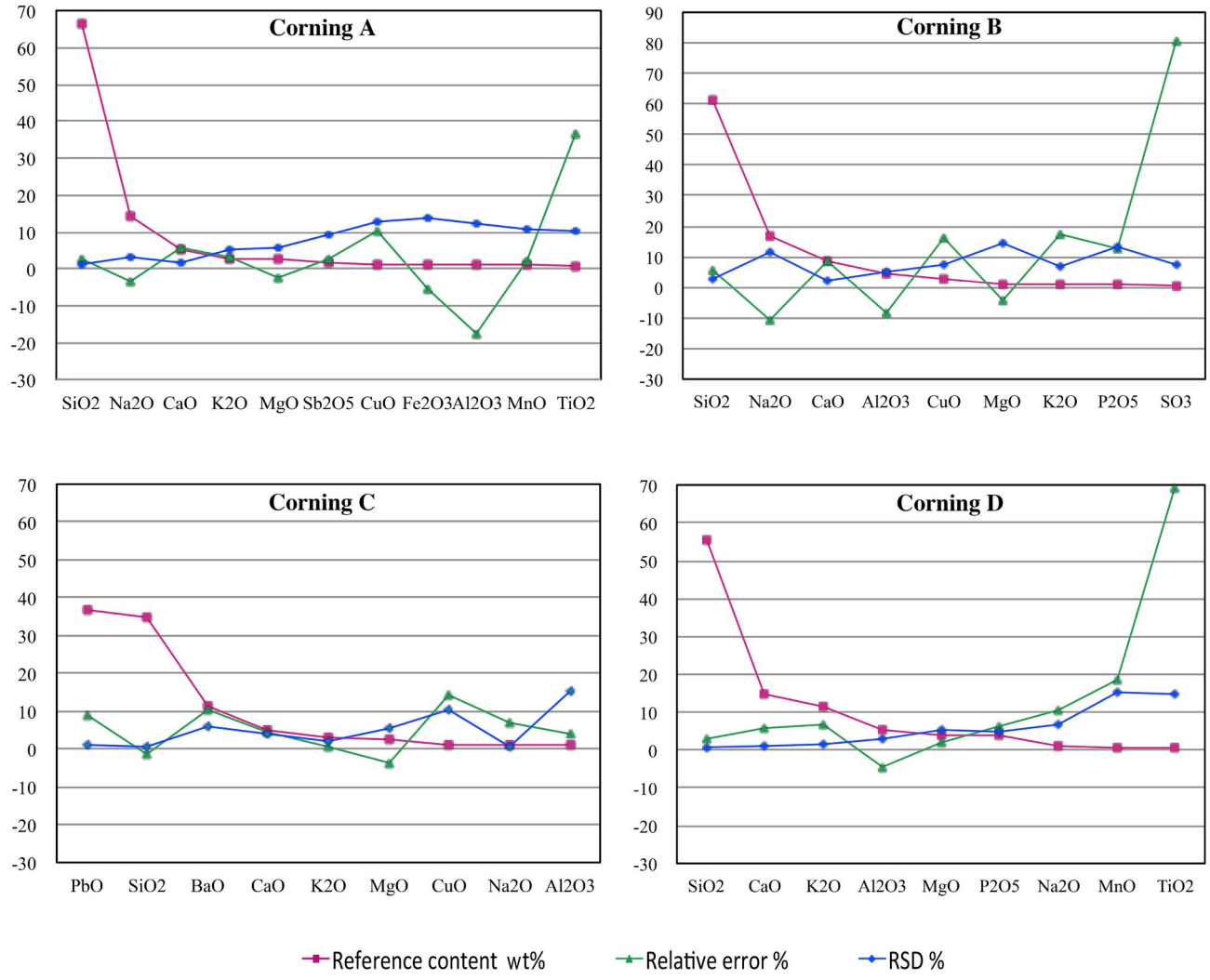

Fig. 5. Accuracy and precision of SEM-EDS analyses on Corning glass standards.

3. Data generation and quality control

The majority of samples were analysed using scanning electron microscopy with energy dispersive spectrometry (SEM-EDS), and a few by Laser Ablation Inductively Coupled Plasma-Mass Spectrometry (LA-ICP-MS).

The SEM-EDS analyses were done on polished cross-sections at the Wolfson Archaeological Science Laboratories at the UCL Institute of Archaeology, using a JEOL JSM-35CF, in two runs in 2011 and 2012. The instrument was operated at 20 kV and 5 nA. Results of the tests on four Corning glass standards with SEM-EDS are given in Fig. 5 and Appendix B. For all reference glasses, accuracy is usually better than 20% except for SO_3 and TiO_2, while precision is often better than 10% except for Fe_2O_3, Al_2O_3 and MnO, for which it is still better than 15%.

SEM-EDS analyses focused on Inter-Particle Glass (IPG) where possible, usually with an area scanning at magnification from 150 × to 600 × at least on three different parts in a single sample; occasionally a spot analysis was done at higher magnification up to 800 × to avoid interference from adjacent quartz particles which would inflate silica levels. For very small mineral inclusions, spot analysis at up to 1000 × was done. Since the following discussion will focus primarily on the Na/K ratio rather than their absolute contents, data obtained by spot analysis was retained together with that obtained by area scanning, despite the known phenomenon of partial alkali loss during spot analysis.

Loss of alkali due to weathering is a known and serious problem of faience analyses, due to the often very thin glaze layer (Fig. 6a) further exacerbated by a very thin bead wall (Fig. 6c). The typically low content of stabilizing oxides in the glass phase, particularly CaO, MgO and Al_2O_3, further compounds the weathering problem.

According to the established laboratory procedures in the Wolfson Archaeological Science Laboratories at the UCL Institute of Archaeology, usually an analytical total ranging from 98 to 102 wt% before normalization should be expected. However, except for one sample from Shangsunjiazhai (QDS11-2, Fig. 6b) and three from Yujiawan (including 84CYM19-1:1-3, Fig. 6d), none of the analyses met this criterion. Even in those samples with abundant remaining glass phases, and after almost every IPG occurrence had been analysed, most of the totals ranged only from 90 to 95 wt%, with some even below 90 wt%. In these analyses (Appendix C), we noted a tendency for analyses with low analytical totals to have lower total alkali content, and those with lower alkali content to have increased chlorine content. Both increased chlorine content and lower analytical totals through loss of alkali oxides are indicators of incipient glass corrosion prior to the total

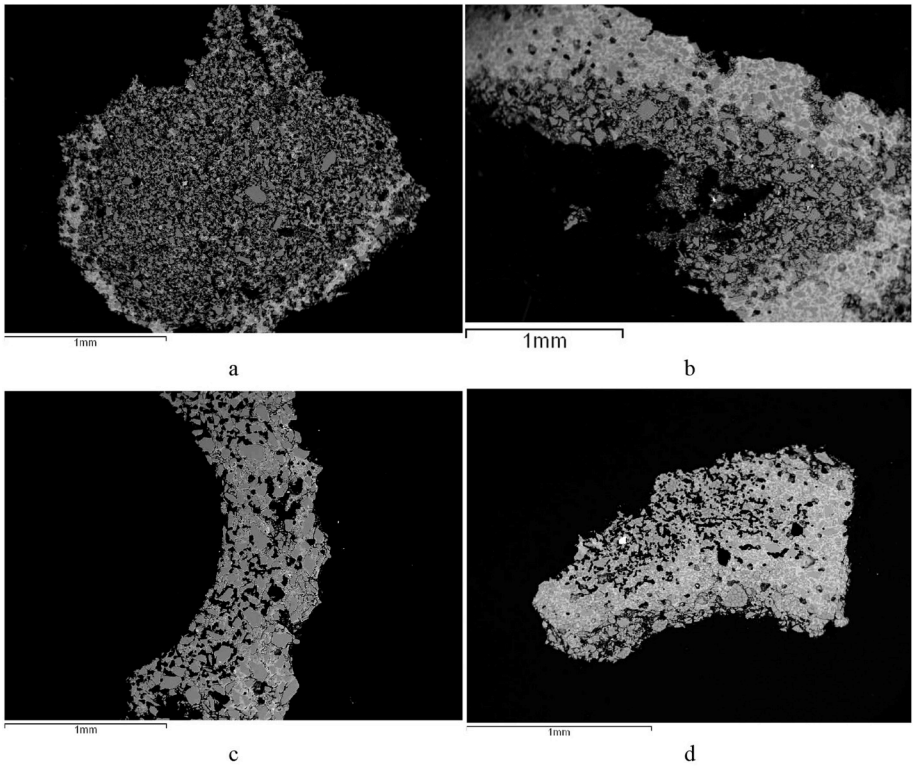

Fig. 6. SEM photomicrographs of polished sections: a) sample TB4 showing a rather thin IAL (interaction layer) over a quartz body without a glaze layer left; b) sample QDS11-2 showing abundant IPG; c) sample SYD1A showing very limited IPG in the bodies; d) sample CYM19–1:1 showing substantial amount of IPG in the body. BSE images showing glass phase as light grey continuous areas.

collapse of the glass network. To test whether the ratio between soda and potash is affected by this incipient corrosion we plotted the alkali ratio against total alkali content (Fig. 7).

Faience with a soda to potash ratio in the glaze significantly above 1.5 is regarded as soda-rich (Fig. 7a), while mixed alkali faience is typically defined as having a ratio of 0.5–1.5 (Vandiver, 2008: 42); in our data set, those with a slightly higher ratio can also be classified in this mixed alkali category (Fig. 7b). The Na/K ratio of soda-rich faience is more sensitive to the loss of alkalis than that of mixed alkali samples. For soda-rich faience, minimum total alkali levels above 4 wt% should be present; for lower concentrations, the Na/K ratio would drop into the mixed alkali range. Thus, typically only for total alkali levels above 6–7 wt% a safe classification can be made. For most mixed alkali faience, again a minimum total of alkalis above 4 wt% is necessary to avoid a risk of distorted classification due to soda depletion, while a total alkali content around 6–7 wt% or more is necessary for a reliable classification. Based on this understanding how the alkali ratio is affected by the partial loss of alkalis, we decided to select three to five analyses for each sample which have a minimum of 90 wt% analytical total, and ideally around 95 wt% analytical totals and above 7 wt% combined soda and potash as raw results. These were then averaged and reported as final results. Four samples (QDS10-1, QDS11-1, SYD1A, SYD3A) had just one or two analyses matching these criteria, but as they were actually averaged from three repeated analyses for each area with remarkable consistency, they are still reported here.

High potash faience was first identified by Brill from Shaanxi as having predominant potassium with very low magnesia (Brill, 1989), but there has been no clear statement of its defining Na/K ratio. Sample TB1-3 is a mixed-alkali faience bead with an alkali ratio of between 0.8 and 1.4 in the IPG, while the ratio in well-preserved (total alkali above c 12 wt%) IAL analyses is between 0.4 and 0.7. Even in more weathered areas of the IAL the ratio did not fall below 0.3 for individual analyses (Fig. 7b). Therefore, to distinguish weathered mixed alkali faience from high potash ones, we set a criterion for the latter to have a Na/K ratio below circa 0.4 on average at a total alkali content of at least 7 wt%. The above data selection process is not ideal, but that is all what we can do with the weathered material in this study.

The LA-ICP-MS analyses were carried out on complete beads without further preparation at the Institute de Recherche sur les Archéomatériaux (IRAMAT), Centre de la Recherche Scientifique (CNRS) in Orléans in one run in 2011. The instrument was a Nd: YAG pulsed laser with a wavelength of 266 nm, using 70 s for ablation (20 s for pre-ablation and 50 s for analysis) and 6–8 Hz laser pulse frequency. Typical argon gas flow rate values ranged from 1.15 to 1.35 L/min. The concentrations were calculated according to an established analytical protocol (Gratuze, 2016). Results of the tests on Corning reference B, C, D and NIST SRM 610 with LA-ICP-MS are given in Fig. 8 and Appendix D. For all Corning references, precision (as expressed by Relative Standard Deviation) of major oxides is typically better than 10% except for Cl, while the accuracy (as expressed by relative error) of major oxides is usually better than 10% except for P, Cl and Pb for which it is still mostly better than 20%. For Corning C, accuracy of Ca is worse than 40%, a known but unexplained anomaly for that sample and not repeated for other reference materials (Gratuze, pers. com.).

4. Results

4.1. Raw materials

SEM-EDS and LA-ICP-MS results are listed in Table 3 and Table 4. Based on the above criteria our analyses fall in three groups: rich in potash, mixed-alkali based, and soda-rich plant-ash based (Fig. 9).

The three beads from Shangsunjiazhai (Kayue, QDS7A, QDS10-1 and QDS11-1) and both from Dahekou (SYD1A, SYD3A) that have a

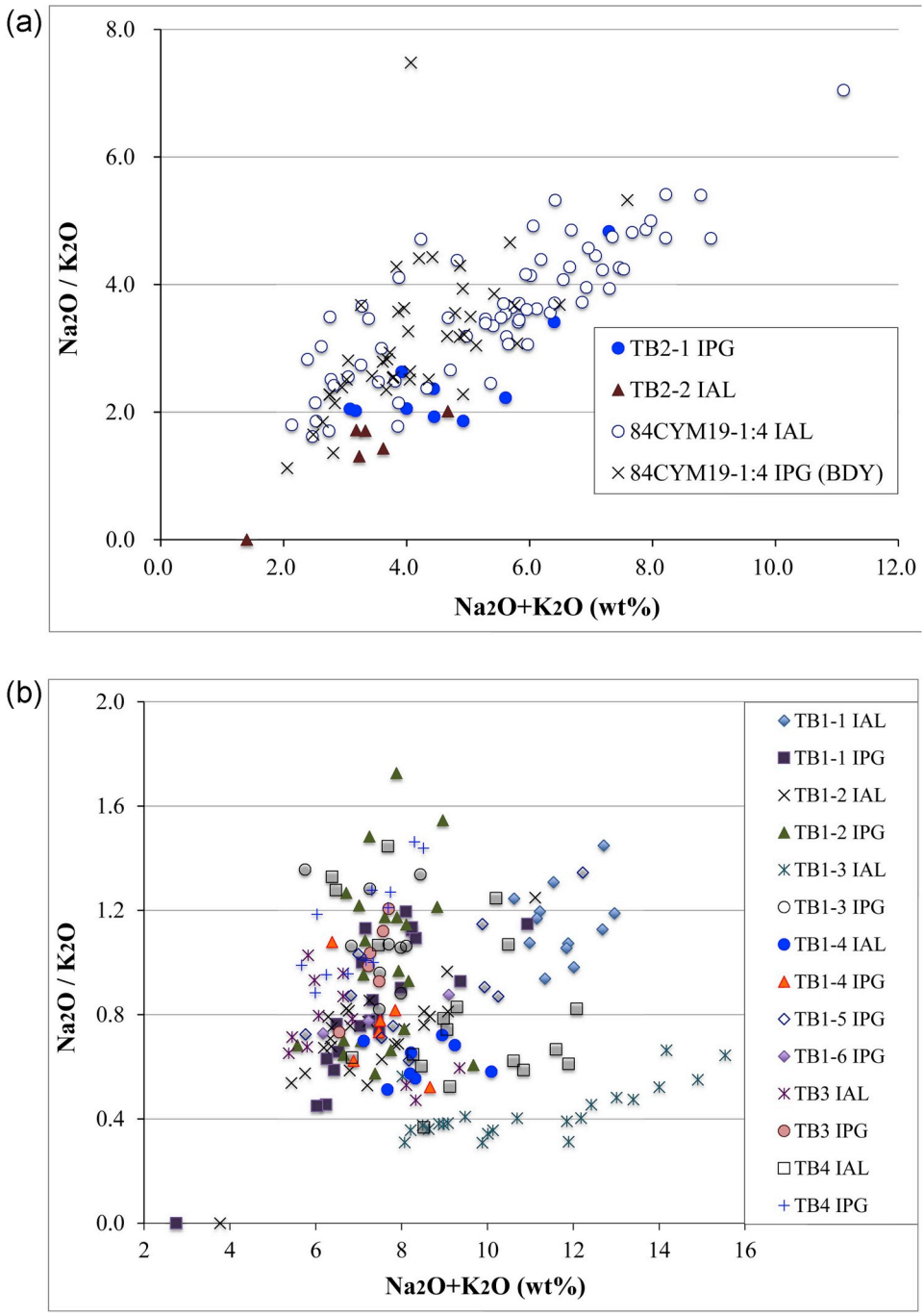

Fig. 7. Total alkali contents vs the ratio of soda to potash showing all individual analyses on several samples with abundant glass phases, to show how loss of alkalis affected the Na/K ratio: a) soda-rich samples; b) mixed alkali samples.

significantly greater potash content than soda content are low in calcium and magnesium (Fig. 10 a), typical for Chinese faience of Western Zhou (Lei and Xia, 2015). The potash-rich sample from Shangsunjiazhai (Tangwang, QDS9A) very likely belongs to the same category, as its calcium and magnesium are both below detection limit, indicating a continuous circulation or production of this compositional type of faience in this area for a long time. Based on the very low impurities in glass phases, Brill hypothesised that either purified vegetal ash or saltpetre (potassium nitrate) was used as flux for these (Brill, 1989). The presence of zirconium in QDS7A, QDS9A and QDS11-1 and the presence of monazite in SYD3A indicate the use of sand for these three sub-groups of faience, even though they show a quite loose range in alumina and iron oxide content (Fig. 10 b). They might share the same recipe of raw materials, but based on such limited data it is hard to determine whether the sand came from the same region.

One sample from Shangsunjiazhai in Qinghai province (Kayue,

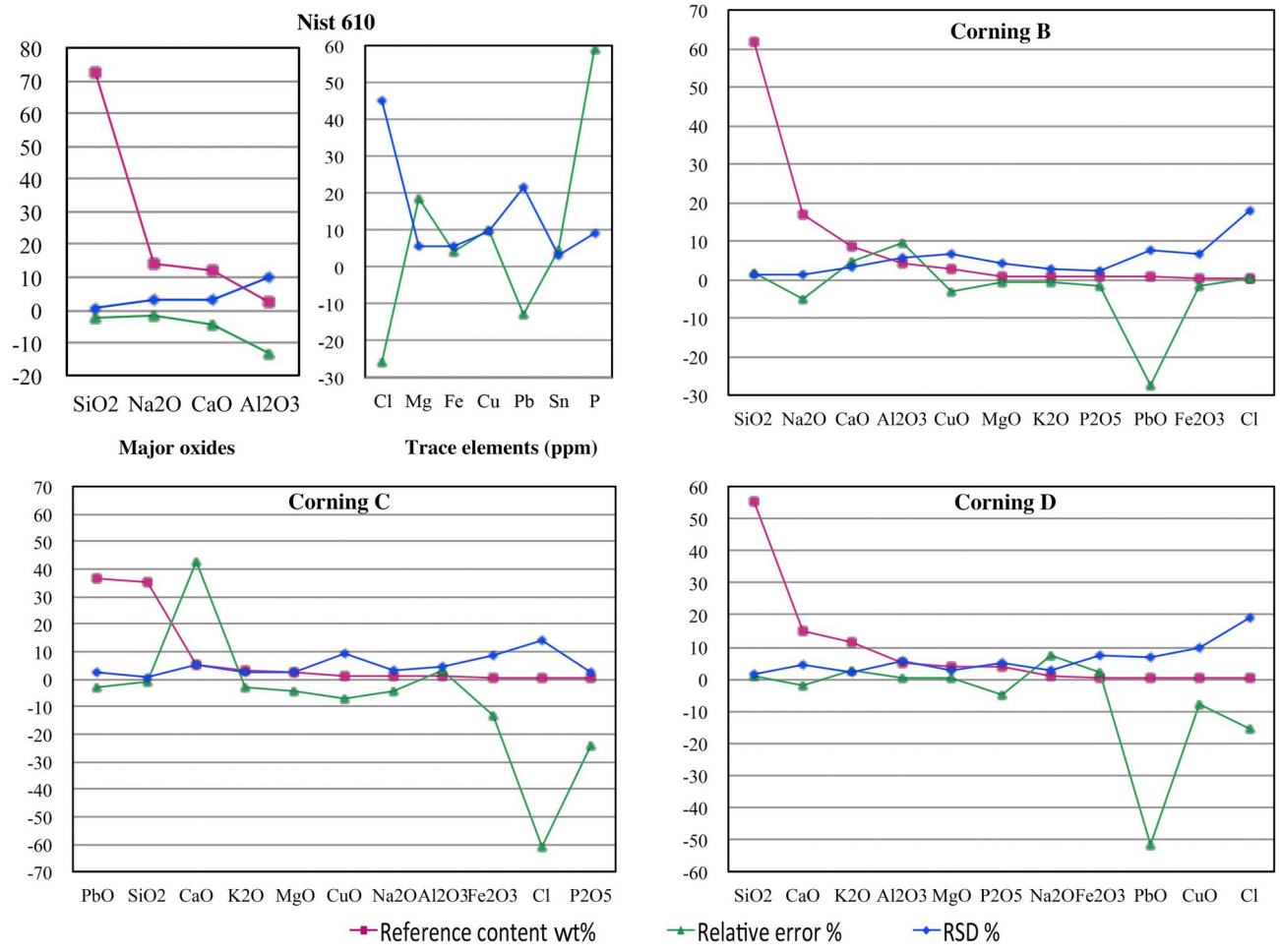

Fig. 8. Accuracy and precision of LA-ICP-MS analyses on NIST 610 and Corning glass standards.

QDS11-2) and the majority of Tianshanbeilu samples are mixed-alkali based. However, the Qinghai sample has much lower content in both magnesia and calcium oxide than the Xinjiang samples (Fig. 10 a). Furthermore, although the presence of zirconium in QDS11-2 and the presence in the Tianshanbeilu samples of some inclusions such as diopside, feldspar and others rich in iron oxide or alumina suggest sand as raw material for both sub-groups, they differ in iron (Fig. 10 b, see also the significant differences in Na/Mg and Na/Ca in Table 3), indicating that they are from different source origins.

In accordance with an earlier study (Zhang and Ma, 2009), our analyses on all three samples from tomb M19 at Yujiawan (84CYM19–1:1, −1:3 and −1:4) demonstrate that they were made from soda-rich plant ash. Zircon, monazite and feldspar have been observed frequently in all samples, indicating the use of quartz sand. Two samples from Tianshanbeilu (TB2-1, −2) and the only sample from M113 of Tianma-Qucun (SJH3) are badly weathered so that their total alkali is very low (Table 3). But even at such low levels soda is still twice the potash level, thus strongly indicating an originally very soda-rich composition. The two soda-rich samples from Tianshanbeilu (Fig. 7 a) have similar level in magnesia, calcium and iron oxide and alumina as the mixed-alkali ones from the same cemetery (Fig. 10), potentially indicating that all the Tianshanbeilu faience might have the same provenance even when using a different flux.

4.2. Colorants

All the investigated samples are coloured by copper, in common with published analyses. Trace element data of metals related to copper are rare due to instrumental constraints (e.g., Lei and Xia, 2015); however, Brill et al. (1991) report high lead content in some Zhou period faience beads. The three beads from tomb M19 at Yujiawan (84CYM19–1:1, −1:2 and −1:3) had already been analysed using SEM-EDS, and the LA-ICP-MS analyses yielded closely matching data. The average concentration of copper oxide was determined as 8.2 wt% (SEM-EDS) and 6.6 wt% (LA-ICP-MS), respectively. The corrected average LA-ICP-MS values for tin (*c.* 750 ppm) and lead (*c.* 8000 ppm), which are equivalent to an original copper alloy with around 1 wt% tin and *c.* 10 wt% lead, point to the use of leaded copper with a low tin content as the raw material for the colorant. The bead from M113 of the Jin State cemetery (SJH3) was probably coloured by leaded copper (see Table 3), with a ratio of lead oxide to copper oxide of 0.4.

4.3. Glazing methods

No quartz-free glaze layer is present in any of the samples. For some samples it is hard to determine whether the fragment represents the IAL or the body due to the random nature of fragments peeling off (Fig. 6 b),

Table 3
Average concentrations of major and minor oxides in the faience investigated in this paper, analysed by SEM-EDS (wt%).

Alkali type	Code	Component	SiO_2	Na_2O	K_2O	CaO	MgO	Al_2O_3	FeO	CuO	Pb	Cl	Na/K	Analytical total	Na/Mg	Na/Ca
High potash	QDS7A	IPG	81.1	1.62	7.07	0.65	0.44	4.16	0.51	3.07	bd	0.53	0.23	96.9	3.69	2.49
High potash	QDS9A	IPG	78.7	2.42	10.1	bd	bd	1.96	0.11	5.92	bd	0.52	0.24	98.9	n/a	n/a
High potash	QDS10-1	IPG	82.6	1.74	6.69	0.25	0.20	2.30	1.28	4.42	bd	0.27	0.26	95.8	8.74	7.06
High potash	QDS11-1	IPG	80.1	2.21	9.19	0.32	0.33	6.29	bd	1.75	bd	bd	0.24	94.7	6.64	6.89
High potash	SYD1A	IPG	84.6	0.80	6.39	0.58	0.51	4.80	0.37	1.84	bd	0.15	0.13	97.3	1.56	1.39
High potash	SYD3A	IPG	75.2	3.15	10.1	1.43	0.54	3.38	0.92	4.75	bd	0.51	0.31	97.1	5.88	2.20
Mixed-alkali	TB1-1	IAL	70.3	6.73	5.65	2.01	0.95	1.91	1.52	10.0	bd	0.84	1.19	94.9	7.12	3.34
Mixed-alkali	TB1-1	IPG(BDY)	71.7	5.15	4.89	2.36	1.18	2.17	1.77	10.3	bd	0.52	1.05	95.1	4.37	2.18
Mixed-alkali	TB1-2	IAL	69.5	5.12	5.05	2.25	0.97	2.06	1.34	12.5	bd	1.15	1.01	94.1	5.25	2.27
Mixed-alkali	TB1-2	IPG(BDY)	73.4	5.04	3.90	2.07	0.93	2.10	1.82	9.90	bd	0.82	1.29	96.5	5.42	2.44
Mixed-alkali	TB1-3	IAL	69.0	6.00	9.72	1.88	0.78	1.33	1.19	9.55	bd	0.54	0.62	94.5	7.66	3.18
Mixed-alkali	TB1-4	IAL	72.1	3.73	5.76	2.27	1.16	2.23	1.32	10.6	bd	0.85	0.65	95.8	3.22	1.64
Mixed-alkali	TB1-4	IPG (BDY)	73.1	3.50	4.51	2.44	1.09	2.61	1.68	10.4	bd	0.66	0.78	94.9	3.22	1.44
Mixed-alkali	TB1-5	IPG	69.3	5.81	5.60	2.35	0.97	2.18	1.79	11.1	bd	0.82	1.04	94.6	5.98	2.47
Mixed-alkali	TB1-6	IPG	71.3	3.56	4.45	2.13	1.03	2.25	1.57	12.4	bd	1.03	0.80	93.7	3.44	1.68
Mixed-alkali	TB3	IAL	73.6	3.27	6.13	2.02	0.87	2.09	1.18	10.4	bd	0.65	0.53	91.5	3.77	1.62
Mixed-alkali	TB3	IPG (BDY)	74.4	4.15	3.85	2.23	0.76	2.98	1.88	9.41	bd	0.32	1.08	94.8	5.44	1.86
Mixed-alkali	TB4	IAL	73.3	4.45	5.96	2.01	1.01	1.81	1.40	9.73	bd	0.41	0.75	94.7	4.42	2.21
Mixed-alkali	TB4	IPG (BDY)	72.6	5.08	3.65	2.20	1.15	2.75	1.40	10.7	bd	0.46	1.39	93.7	4.43	2.31
Mixed-alkali	QDS11-2	IPG	74.0	6.92	9.15	0.55	0.27	2.52	0.13	6.08	bd	0.36	0.76	99.0	25.2	12.7
Soda-rich plant ash	84CYM19-1:1	IAL	72.8	11.5	2.87	0.49	0.47	2.43	0.88	8.05	bd	0.81	4.02	100.8	24.8	23.4
Soda-rich plant ash	84CYM19-1:1	IPG (BDY)	74.8	9.79	2.72	0.55	0.51	2.55	0.99	7.63	bd	0.50	3.60	102.5	19.2	17.8
Soda-rich plant ash	84CYM19-1:3	IAL	76.1	10.4	2.75	bd	bd	2.67	1.08	6.51	bd	0.40	3.78	102.2	n/a	n/a
Soda-rich plant ash	84CYM19-1:3	IPG (BDY)	75.6	10.6	2.60	bd	bd	3.14	0.89	7.16	bd	bd	4.07	102.6	n/a	n/a
Soda-rich plant ash	84CYM19-1:4	IAL	72.2	8.35	1.54	0.88	bd	2.00	1.24	10.2	2.43	1.01	5.43	91.6	n/a	9.51
Soda-rich plant ash	84CYM19-1:4	IPG (BDY)	74.7	5.22	1.40	1.05	0.68	2.62	1.24	9.45	2.14	1.69	3.73	91.5	7.72	4.96
Very likely soda-rich	TB2-1	IPG	73.3	5.47	1.63	2.67	0.71	2.30	1.26	11.2	bd	1.21	3.35	90.6	7.76	2.05
Very likely soda-rich	TB2-2	IAL	75.8	2.56	1.40	2.76	0.96	2.46	1.78	10.8	bd	1.29	1.83	93.7	2.66	0.93
Very likely soda-rich	SJH3	IPG	84.4	2.04	1.03	0.40	0.44	3.32	0.53	4.62	1.81	0.74	1.98	95.5	4.64	5.10

Table 4
Average concentrations of major and minor oxides of Yujiawan samples analysed by LA-ICP-MS.

Code	SiO_2	Na_2O	CaO	K_2O	MgO	Al_2O_3	Fe_2O_3	CuO	P_2O_5	Cl	PbO	SnO_2
CYW 1	95.9	0.15	0.27	0.21	0.14	1.03	0.19	1.57	0.09	0.29	0.0440	28
CYW 2	95.6	0.19	0.45	0.23	0.11	0.81	0.19	1.77	0.16	0.35	0.0230	33
CYW 3	93.9	0.33	0.53	0.09	0.09	0.56	0.16	3.10	0.14	0.99	0.0312	12
CYW 4	95.8	0.22	0.81	0.24	0.15	0.84	0.24	0.98	0.40	0.23	0.0336	8
84CYM19-1:1	82.9	5.37	0.86	1.39	0.33	2.11	0.58	3.04	0.10	2.87	2.62	200
84CYM19-1:3	88.8	4.83	0.20	1.11	0.10	1.36	0.44	2.50	0.04	0.21	1.77	606
84CYM19-1:4	83.4	7.89	0.51	0.63	0.15	0.97	0.54	4.30	0.19	0.47	7.83	320

making it also difficult to evaluate the glazing method based on differences between IPG-BDY and IAL glass compositions (see e.g. Rehren, 2008). The samples from Tianshanbeilu, Shangsunjiazhai and Dahekou have little interstitial glass in the bodies (Fig. 6 a-c), suggesting that a cementation method was used to create these thin-walled beads. Only Tianshanbeilu samples have their IAL preserved, but soda and potash concentrations did not always increase or decrease from the IAL to the body (Table 3). Some increases or decreases could also be due to heterogeneity across a whole sample, as our analyses have shown (Appendix C). All three samples of Yujiawan (84CYM19) have sufficient inter-particle glass to bond together adjacent quartz particles, and the bodies also contain more or less continuous interstitial glass, indicating that they are glazed by efflorescence (Fig. 6 d).

5. Discussions

Soda-rich faience is generally thought to be made in or influenced by Egypt or Western Asia (e.g., Zhang and Ma, 2009; Lei and Xia, 2015). Our SEM and LA-ICP-MS analyses have shown that some of the soda-rich faience was coloured by a leaded copper alloy, which has no correspondence in soda-rich plant ash faience either from the Middle East or Egypt, while such alloys were widely used in Central China. We therefore cannot exclude the possibility that theses soda-rich faience beads with relatively high lead oxide were locally made, a possibility already raised by Brill et al. (1991: 117) for several other Zhou period faience beads. Accordingly, during the early to middle period of the Western Zhou period, Chinese people might have experimented with

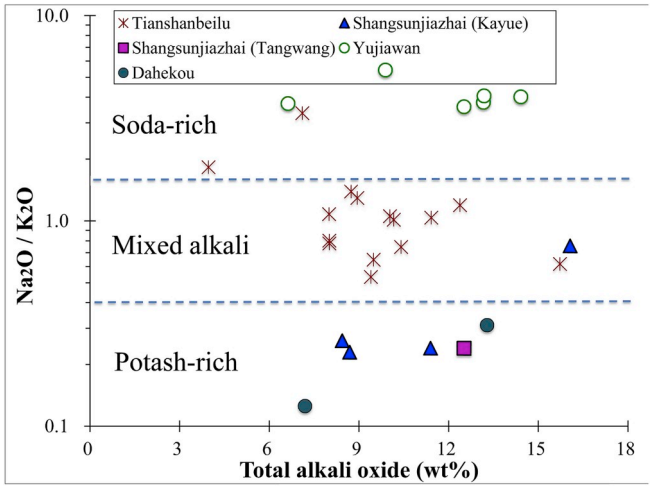

Fig. 9. Total alkali contents vs the ratio of soda to potash of the three compositional groups, namely soda-rich plant ash samples with ratios above circa 1.5, for the mixed-alkali samples (those with ratios ranging from 0.5 to 1.5), and potash-rich samples with ratios below circa 0.4. Where a sample gave data for IAL as well as IPG these were plotted separately. Note the logarithmic scale of the Y axis.

faience making using soda-rich desert plant ash similar to that used in Western Asia and Egypt.

Furthermore, our new analyses identified several high-potash beads from Kayue Culture contexts in eastern Qinghai, pre-dating the previously published high-potash faience beads. They displayed some characteristic features that are typically found among potash-rich faience from Jin-Shan area, supporting the hypothesis of a long lasting and widely established local Chinese production of high-potash faience. Although the origins of high-potash faience making in eastern Qinghai and of soda-rich plant ash faience making in Jin-Shan cannot be addressed yet, it seems that the Zhou people witnessed technological change in faience making, resulting in a common high potash recipe, along with some morphological preferences shared with the Kayue people.

Ten samples, representing the only four faience beads from Tianshanbeilu found among nearly 5,500 stone beads (see above), turned out to be made using two different types of flux, mixed alkali and soda-rich plant ash. We propose that they are very likely occasional imports rather than locally produced. The use of mixed alkali faience first emerged in South Russia and then spread from there during the 2nd millennium BC to Europe (Angelini, 2008: 129). Meanwhile, soda-rich composition was also detected among the earliest faience beads from this region (Shortland et al., 2007). Some specific morphologies, e.g. long smooth tubes, tubes with ribbed ornamentation or segmented tubes, and tubes with wart-like or horn ornamentation first appeared in the northern Caucasus. They borrowed their shapes from beads made from other materials used earlier in this region, indicating a local origin of these typologies (Shortland et al., 2007). Therefore, the rare Tianshanbeilu mixed alkali beads, in the shape of either long or segmented tubes, show a very close link with the North Caucasus region and the Eurasian steppe. During the Bronze Age, beads of these two shapes, made either of bronze or faience (often called 'paste beads'), were quite popular in the Semirechye region of Central Asia (Goriachev, 2004); however, no analytical results on these faience beads have yet been published, which prevents us from further comparison. Considering the very close relationship between western Xinjiang and the Semirechye region during the Bronze Age (Yang et al., 2016: 120), it is likely that these foreign beads were introduced into Xinjiang from Central Asia. The same is likely the case for the earliest faience from China published so far, a string of segmented tubes from Saensayi in northern Xinjiang, and also those later ones found from Ya'er that have been recently re-analysed with SEM and found to be mixed alkali (Liu Nian, pers. com.).

Early faience beads are relatively rare in Xinjiang compared to Qinghai and Jin-Shan, making it hard to propose a local manufacture.

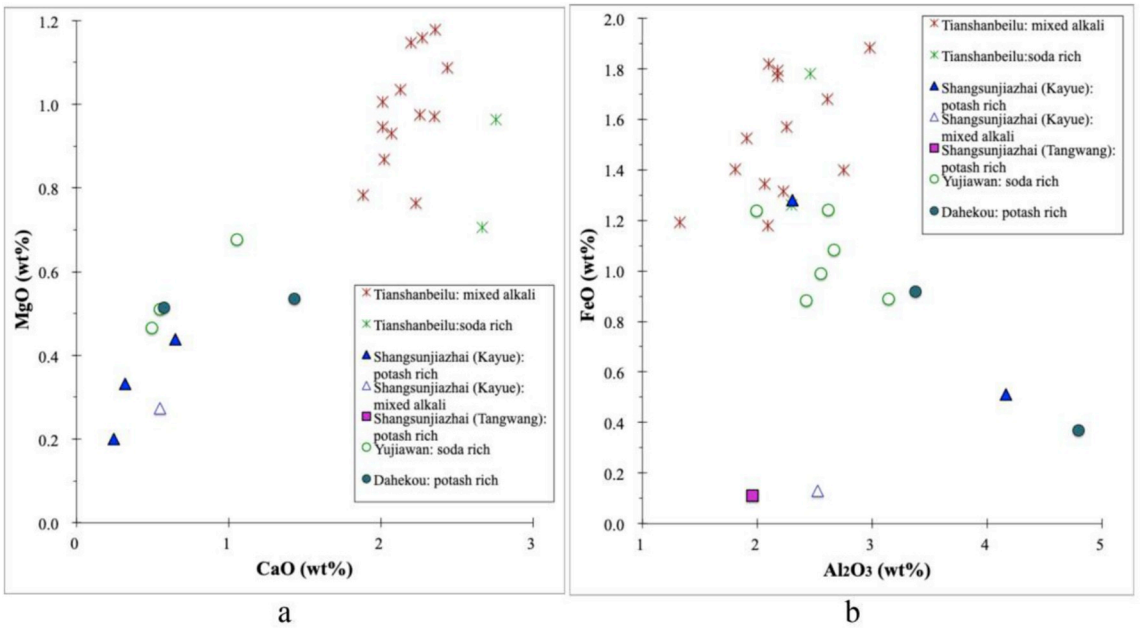

Fig. 10. a) MgO vs CaO of IPG, by site and alkali type; b) iron oxide vs alumina, by site and alkali type.

As noted above, both the mixed alkali and soda-rich plant ash faience from Xinjiang differed both in typology and in compositional features from their parallels from Qinghai and Yujiawan. Therefore, at present it seems that eastern Xinjiang did not contribute too much to the faience production that developed in eastern Qinghai and the Jin-Shan region.

6. Conclusions and outlook

The emergence of faience beads in China is an important subject of study closely related to the cultural interaction of China with the outside world, both in terms of exchange of materials, the communication of ideas of value and beauty, and the spread, adaption and development of specialised technologies. Our work presented here provides for the first time well-dated evidence for the use of faience in Xinjiang during the middle and the second half of the second millennium BC, made using mixed-alkali and soda-rich plant ashes and with a likely production origin of the beads in the north Caucasus or the Steppe. These beads, typologically and compositionally closely similar to beads circulating outside China, were most likely imported from Central Asia and remain rare finds. In the second half of the second millennium and the early first millennium BC we see the use first of locally-produced soda-rich faience and then of high-potash faience across a wide region of northern and north-western China, from eastern Qinghai through eastern Gansu to Shaanxi and Shanxi, indicating the existence at the time of an established and diverse faience industry within the cultural heartland of China. The technology has been adopted to use locally available raw materials. During the early period of Western Zhou, there appears to have been an experimental period for faience manufacture by Zhou people at the border region of the Central Plains. In particular, some of the fluxes are materially different from the classical soda-rich or mixed-alkali plant ashes used in Western and Central Asia, even though we still do not know the exact nature of the potash-rich raw material(s). From the middle Western Zhou, we see the regular use of quintessentially Chinese raw materials both in the fluxes (high potash) and the colorants (leaded copper). It is reasonable to assume that the Zhou people learnt these techniques or perfected their own by contact with their neighbours in the west, e.g. the Kayue people of Qinghai Province, who were the first to use high-potash glaze recipes. However, the available data is still too sketchy to properly discuss the origin of either the soda-rich plant ash faience making in the Zhou realm, or the high potash one in Qinghai.

Future work would benefit from the more systematic determination of trace elements using LA-ICP-MS in well-dated finds. In the bodies, emphasis should be on the presence of specific minerals that may help define groups of compositionally similar beads, and potentially constraining their geological source regions. Detailed analysis of better-preserved glaze matrices and their colorants will help identifying the nature and selection of raw materials as a reflection of human agency and technological styles; together with an identification of the production technologies this will help characterise specific workshop traditions, their adaptation to new raw materials, and the emergence of new lineages of technological and morphological styles. The limited data available so far already indicates that much can be learned from a broader and more reliable body of data from well-dated objects, even when restricting the invasive analysis to small fragments. Of particular interest is the determination of the relative proportions of copper, lead and tin to test whether the faience beads found in China have systematically different alloy signatures from those of Central Asia and further West. A specific avenue within this future research should include the determination of lead isotope abundance ratios, to test for any links between the copper used as colorant and the contemporary bronze industry. Here, much work is recently shedding increasing light on the provenance of copper and lead from late Shang and early Western Zhou bronzes in the Chinese heartland, and linking future faience research to this could prove highly informative.

Acknowledgements

The research was done while the first author was a Newton Fellow at the UCL Institute of Archaeology, hosted by the second author. The financial and academic support through the Newton International Fellowship from the British Academy and the National Key Research Base for Humanities and Social Sciences under the Ministry of Education of China (Grant No. 16JJD780010) are gratefully acknowledged. Samples were kindly made available for analysis by Kurban Rahman at the Hami Museum, Li Zhi-Xin and Qiao Hong from the Qinghai Institute of Archaeology, Xie Yao-Tin from Shanxi University and Ji Kun-Zhang at the Shanxi Institute of Archaeology. Kevin Reeves' assistance with sample preparation and SEM-EDS analysis is acknowledged. Bernard Gratuze kindly provided the LA-ICP-MS data on seven beads from Yujiawan. Discussions with Robert Brill, Lu Lian-Cheng and Liu Nian have greatly contributed to our understanding of these beads and are highly appreciated. Comments from four anonymous reviewers have helped us to strengthen our argument; any remaining shortcomings are our own responsibility.

Appendix A. ^{14}C dates from Shangsunjiazhai cemetery of 'Tangwang type' (Institute of Archaeology, Chinese Academy of Social Sciences, 1991)

Tomb number	Sample type	Laboratory code	Dendrochronolocially calibrated date
M333	Coffin wood	BK77014	BC 1211–915
M979	Wood	BK80011	BC 796–432
M989	Wood	BK80012	BC 766–402
M1042	Wood	BK80013	BC 825–595
M1046	Charcoal	BK80014	BC 1266–1008

APPENDIX B

Reference	Oxide	SiO_2	Al_2O_3	Fe_2O_3	Na_2O	MgO	K_2O	CaO	PbO	CuO	CoO	SnO_2	Sb_2O_5	MnO	TiO_2	BaO	ZnO	P_2O_5	SO_3	Cl	NiO	SrO	V_2O_3
Corning A	Test Wt%	68.43	0.83	1.03	13.83	2.60	2.96	5.33		1.29			1.80	1.02	1.08								
	Reference content Wt%	66.56	1.00	1.09	14.3	2.66	2.87	5.03	0.12	1.17	0.17	0.19	1.75	1.00	0.79	0.56	0.044	0.13	0.54	0.20		0.10	
	Absolute error Wt%	1.87	-0.18	-0.06	-0.47	-0.06	0.09	0.30		0.12			0.05	0.02	0.29								
	Relative error %	2.80	-17.50	-5.50	-3.31	-2.34	3.14	5.94		10.45			2.64	2.00	36.71								
	RSD %	1.21	12.21	13.83	3.02	5.58	5.42	1.52		13.01			9.43	10.91	10.48								
Corning B	Test Wt%	65.23	4.00		15.17	0.985	1.177	9.292		3.085								0.926	0.885				
	Reference content Wt%	61.55	4.36	0.34	17.0	1.03	1.00	8.56	0.61	2.66	0.046	0.04	0.46	0.25	0.089	0.12	0.19	0.82	0.49	0.20	0.099	0.019	0.036
	Absolute error Wt%	3.68	-0.36		-1.83	-0.05	0.18	0.73		0.43								0.11	0.40				
	Relative error %	5.97	-8.18		-10.76	-4.37	17.67	8.55		15.98								12.93	80.61				
	RSD %	2.89	5.10		11.50	14.53	6.81	2.21		7.17								13.20	7.19				
Corning C	Test Wt%	34.34	0.91		1.15	2.66	2.86	5.31	39.89	1.29						12.59							
	Reference content Wt%	34.87	0.87	0.34	1.07	2.76	2.84	5.07	36.7	1.13	0.18	0.19			0.79	11.4		0.14	0.54	0.20		0.29	
	Absolute error Wt%	-0.53	0.04		0.08	-0.10	0.02	0.24	3.19	0.16					-0.79	1.19							
	Relative error %	-1.51	4.21		7.01	-3.68	0.82	4.64	8.69	14.16					-100.00	10.42							
	RSD %	0.77	15.02		0.62	5.56	1.90	4.20	1.26	10.37						6.07							
Corning D	Test Wt%	56.89	5.06		1.33	4.03	12.08	15.64						0.65	0.64			4.18					
	Reference content Wt%	55.24	5.30	0.52	1.20	3.94	11.3	14.80	0.48	0.38		0.10	0.97	0.55	0.38	0.51	0.10	3.93	0.54	0.20		0.057	
	Absolute error Wt%	1.65	-0.24		0.13	0.09	0.78	0.84						0.10	0.26			0.25					
	Relative error %	2.98	-4.47		10.65	2.20	6.91	5.67						18.55	69.08			6.25					
	RSD %	0.75	3.17		6.80	5.23	1.62	1.24						15.24	14.68			4.95					

APPENDIX C

	Na_2O/K_2O	Na_2O+K_2O	Totals before normalised	Cl
TB1-1 IAL	1.08	11.0	93.2	0.99
TB1-1 IAL	1.20	11.2	94.5	0.82
TB1-1 IAL	1.45	12.7	94.3	0.92
TB1-1 IAL	1.31	11.5	95.9	0.71
TB1-1 IAL	1.17	11.2	93.2	1.22
TB1-1 IAL	1.13	12.7	93.4	0.81
TB1-1 IAL	1.07	11.9	93.1	1.00
TB1-1 IAL	1.25	10.6	94.8	0.92
TB1-1 IAL	1.19	13.0	94.3	0.75
TB1-1 IAL	0.94	11.3	93.6	1.11
TB1-1 IAL	1.06	11.8	94.7	0.98
TB1-1 IAL	0.98	12.0	92.9	0.90
TB1-1 IPG (BDY)	1.12	8.24	96.2	0.32
TB1-1 IPG (BDY)	0.76	6.49	90.4	0.46
TB1-1 IPG (BDY)	0.86	7.33	93.8	0.39
TB1-1 IPG (BDY)	1.09	8.33	95.7	0.32
TB1-1 IPG (BDY)	0.78	7.44	94.3	0.51
TB1-1 IPG (BDY)	0.78	7.27	94.3	0.47
TB1-1 IPG (BDY)	0.90	7.99	94.9	0.57
TB1-1 IPG (BDY)	0.66	6.53	95.4	0.75
TB1-1 IPG (BDY)	1.15	10.9	96.3	0.64
TB1-1 IPG (BDY)	1.13	7.16	94.4	0.51
TB1-1 IPG (BDY)	0.93	9.37	93.2	0.59
TB1-1 IPG (BDY)	0.74	7.48	93.8	0.72
TB1-1 IPG (BDY)	1.00	7.08	93.5	0.71
TB1-1 IPG (BDY)	1.20	8.10	97.8	0.38
TB1-1 IPG (BDY)	0.59	6.43	96.1	0.62
TB1-1 IPG (BDY)		2.75	86.4	0.49
TB1-1 IPG (BDY)	1.13	8.24	96.0	0.49
TB1-1 IPG (BDY)	0.45	6.24	94.0	0.63
TB1-1 IPG (BDY)	0.45	6.03	94.8	0.81
TB1-1 IPG (BDY)	0.76	7.04	94.4	0.93
TB1-1 IPG (BDY)	0.63	6.26	95.9	0.83
TB1-2 IAL	0.79	8.66	91.1	0.92
TB1-2 IAL	0.69	7.84	91.4	1.10
TB1-2 IAL	0.74	8.06	91.8	0.96
TB1-2 IAL	0.63	7.54	92.4	1.12
TB1-2 IAL	0.67	6.19	90.2	1.23
TB1-2 IAL		3.77	88.0	1.16
TB1-2 IAL	0.58	5.75	88.4	1.04
TB1-2 IAL	0.97	9.06	94.6	1.29
TB1-2 IAL	0.77	7.22	92.2	1.25
TB1-2 IAL	0.68	6.36	89.8	1.25
TB1-2 IAL	0.71	6.34	92.6	1.15
TB1-2 IAL	0.82	6.71	91.3	1.06
TB1-2 IAL	0.76	6.80	93.4	0.73
TB1-2 IAL	0.79	6.29	92.7	1.06
TB1-2 IAL	0.82	6.77	92.9	0.84
TB1-2 IAL	0.54	5.43	90.4	1.17
TB1-2 IAL	0.75	6.37	91.9	1.08
TB1-2 IAL	0.69	7.92	92.9	1.13
TB1-2 IAL	0.85	7.25	92.5	0.65
TB1-2 IAL	0.81	9.08	93.2	1.07
TB1-2 IAL	1.25	11.1	94.1	1.07
TB1-2 IAL	0.76	8.52	93.4	1.10
TB1-2 IAL	0.81	8.52	93.5	1.09
TB1-2 IAL	0.59	6.79	93.3	0.98
TB1-2 IAL	0.53	7.20	94.9	1.08
TB1-2 IPG (BDY)	0.95	7.11	95.8	0.51
TB1-2 IPG (BDY)	0.70	6.65	91.4	0.68
TB1-2 IPG (BDY)	0.93	8.16	94.4	0.53
TB1-2 IPG (BDY)	0.61	9.67	90.4	bd
TB1-2 IPG (BDY)	0.68	5.57	91.2	0.47
TB1-2 IPG (BDY)	0.97	7.93	94.3	0.65
TB1-2 IPG (BDY)	1.17	7.61	94.4	0.38
TB1-2 IPG (BDY)	1.17	7.89	93.3	0.34
TB1-2 IPG (BDY)	1.27	6.71	94.1	bd
TB1-2 IPG (BDY)	0.70	7.05	93.2	0.62
TB1-2 IPG (BDY)	1.08	7.15	92.9	0.29
TB1-2 IPG (BDY)	1.55	8.96	97.5	0.9
TB1-2 IPG (BDY)	1.48	7.25	95.9	0.28
TB1-2 IPG (BDY)	1.73	7.88	92.1	bd
TB1-2 IPG (BDY)	1.15	8.11	95.1	0.66

TB1-2 IPG (BDY)	1.22	7.01	93.8	0.38
TB1-2 IPG (BDY)	1.21	8.83	96.9	0.91
TB1-2 IPG (BDY)	0.74	8.06	93.0	0.35
TB1-2 IPG (BDY)	0.66	7.75	92.5	0.51
TB1-2 IPG (BDY)	0.65	6.65	92.9	0.66
TB1-2 IPG (BDY)	0.57	7.38	94.3	0.62
TB1-3 IAL	0.47	13.4	93.5	0.55
TB1-3 IAL	0.48	13.0	92.5	0.58
TB1-3 IAL	0.31	11.9	92.7	0.43
TB1-3 IAL	0.40	12.2	94.5	0.36
TB1-3 IAL	0.66	14.2	93.5	0.59
TB1-3 IAL	0.36	8.63	91.7	0.74
TB1-3 IAL	0.31	8.07	90.1	0.55
TB1-3 IAL	0.38	9.08	92.2	0.57
TB1-3 IAL	0.56	8.02	92.8	0.53
TB1-3 IAL	0.31	9.88	90.3	0.49
TB1-3 IAL	0.36	10.1	92.6	0.40
TB1-3 IAL	0.39	11.9	93.0	0.40
TB1-3 IAL	0.40	10.7	94.6	0.68
TB1-3 IAL	0.45	12.4	93.3	0.48
TB1-3 IAL	0.34	10.0	90.8	0.54
TB1-3 IAL	0.38	8.49	90.9	0.54
TB1-3 IAL	0.36	8.21	90.0	0.45
TB1-3 IAL	0.41	9.48	92.4	0.52
TB1-3 IAL	0.38	8.98	92.9	0.40
TB1-3 IAL	0.38	8.87	91.4	0.90
TB1-3 IAL	0.64	15.5	96.7	0.62
TB1-3 IAL	0.55	14.9	93.4	0.40
TB1-3 IAL	0.52	14.0	93.7	0.35
TB1-3 IPG (BDY)	1.06	6.83	88.5	0.28
TB1-3 IPG (BDY)	1.06	7.98	88.9	0.40
TB1-3 IPG (BDY)	1.28	7.26	92.2	0.33
TB1-3 IPG (BDY)	1.36	5.75	88.5	0.40
TB1-3 IPG (BDY)	1.34	8.44	89.2	0.40
TB1-3 IPG (BDY)	0.88	7.98	85.8	0.67
TB1-3 IPG (BDY)	1.06	8.11	86.1	0.54
TB1-3 IPG (BDY)	1.07	7.70	86.3	0.69
TB1-3 IPG (BDY)	0.96	7.49	87.1	0.47
TB1-3 IPG (BDY)	0.82	7.48	81.5	0.37
TB1-4 IAL	0.68	9.24	95.5	0.93
TB1-4 IAL	0.72	8.95	95.9	1.08
TB1-4 IAL	0.65	8.22	95.6	0.76
TB1-4 IAL	0.56	8.32	94.2	0.88
TB1-4 IAL	0.58	10.1	95.7	0.72
TB1-4 IAL	0.70	7.12	94.4	0.69
TB1-4 IAL	0.51	7.67	92.3	0.87
TB1-4 IAL	0.57	8.20	94.3	0.62
TB1-4 IPG (BDY)	0.82	7.85	95.4	0.59
TB1-4 IPG (BDY)	0.52	8.66	94.0	0.41
TB1-4 IPG (BDY)	1.08	6.38	94.7	0.42
TB1-4 IPG (BDY)	0.73	7.47	94.0	0.74
TB1-4 IPG (BDY)	0.62	6.88	92.5	0.57
TB1-4 IPG (BDY)	0.78	7.50	95.4	0.64
TB1-5 IPG	0.72	5.76	92.7	1.00
TB1-5 IPG	0.76	7.80	92.4	0.77
TB1-5 IPG	0.91	9.93	93.4	0.82
TB1-5 IPG	0.87	10.3	95.4	0.76
TB1-5 IPG	0.71	7.53	94.2	1.06
TB1-5 IPG	1.15	9.88	94.2	0.60
TB1-5 IPG	1.35	12.2	94.9	0.88
TB1-5 IPG	0.87	6.82	93.6	0.92
TB1-5 IPG	1.03	6.99	90.9	0.30
TB1-5 IPG	0.62	8.17	89.9	0.37
TB1-6 IPG	0.78	7.23	92.7	0.83
TB1-6 IPG	0.88	9.10	94.0	1.19
TB1-6 IPG	0.73	6.17	94.4	1.07
TB2-1 IPG	2.05	4.00	89.6	1.42
TB2-1 IPG	2.02	3.17	88.9	1.44
TB2-1 IPG	2.05	3.08	89.6	1.85
TB2-1 IPG	1.86	4.92	90.7	1.27
TB2-1 IPG	2.36	4.44	93.3	0.93
TB2-1 IPG	1.93	4.45	91.1	1.38
TB2-1 IPG	3.41	6.40	91.2	1.25
TB2-1 IPG	4.83	7.29	90.3	1.16
TB2-1 IPG	2.22	5.61	90.2	1.21
TB2-1 IPG	2.63	3.92	90.7	1.25

TB2-2 IAL	1.71	3.33	91.4	1.39
TB2-2 IAL	1.72	3.18	92.4	1.32
TB2-2 IAL	1.31	3.23	92.1	1.53
TB2-2 IAL	2.01	4.67	97.1	1.17
TB2-2 IAL		1.40	91.6	1.46
TB2-2 IAL	1.43	3.62	90.6	1.43
TB3 IAL	0.78	6.85	92.1	0.73
TB3 IAL	0.71	5.45	89.3	0.81
TB3 IAL	0.80	6.07	92.7	0.71
TB3 IAL	0.93	5.97	92.9	0.57
TB3 IAL	0.87	6.64	92.5	0.77
TB3 IAL	0.96	6.64	92.7	1.06
TB3 IAL	0.60	9.35	92.2	0.55
TB3 IAL	0.53	8.11	90.5	0.45
TB3 IAL	0.47	8.33	91.7	0.95
TB3 IAL	0.65	5.37	92.2	1.29
TB3 IAL	0.68	5.80	93.5	0.71
TB3 IAL	1.03	5.82	96.8	1.15
TB3 IPG (BDY)	0.99	7.23	88.4	3.02
TB3 IPG (BDY)	1.21	7.70	95.0	0.35
TB3 IPG (BDY)	1.04	7.27	99.0	0.29
TB3 IPG (BDY)	1.12	7.57	95.0	0.34
TB3 IPG (BDY)	0.73	6.55	93.5	0.60
TB3 IPG (BDY)	0.93	7.48	94.4	0.28
TB4 IAL	0.74	9.06	91.4	0.66
TB4 IAL	0.83	9.29	93.4	0.25
TB4 IAL	1.33	6.38	93.5	0.56
TB4 IAL	1.45	7.68	93.6	0.67
TB4 IAL	1.07	7.46	92.8	0.89
TB4 IAL	0.62	10.6	92.6	0.29
TB4 IAL	1.28	6.47	94.5	0.65
TB4 IAL	0.63	6.85	91.8	1.00
TB4 IAL	0.60	8.46	94.6	0.47
TB4 IAL	0.65	8.27	92.0	0.49
TB4 IAL	1.07	10.5	96.9	0.46
TB4 IAL	0.79	8.98	93.1	0.38
TB4 IAL	0.82	12.1	91.7	0.27
TB4 IAL	0.67	11.6	91.5	0.58
TB4 IAL	0.59	10.8	90.3	0.33
TB4 IAL	0.52	9.12	90.5	0.56
TB4 IAL	1.25	10.2	91.4	0.32
TB4 IAL	0.61	11.9	93.0	0.64
TB4 IAL	0.37	8.52	89.6	0.54
TB4 IPG (BDY)	0.88	5.99	89.8	0.62
TB4 IPG (BDY)	0.99	5.67	93.7	0.66
TB4 IPG (BDY)	1.00	7.34	94.6	0.24
TB4 IPG (BDY)	1.18	6.03	92.6	0.34
TB4 IPG (BDY)	1.28	7.31	93.5	0.31
TB4 IPG (BDY)	1.01	7.17	92.4	0.45
TB4 IPG (BDY)	1.46	8.30	92.9	0.34
TB4 IPG (BDY)	0.96	6.75	96.6	0.5
TB4 IPG (BDY)	1.27	7.74	93.7	0.56
TB4 IPG (BDY)	1.21	7.69	92.3	0.34
TB4 IPG (BDY)	0.95	6.25	92.2	0.27
TB4 IPG (BDY)	1.44	8.51	94.5	0.49
84CYM19-1:4 IAL	3.64	5.71	90.5	1.08
84CYM19-1:4 IAL	5.32	6.42	88.3	0.93
84CYM19-1:4 IAL	3.54	5.61	88.9	0.88
84CYM19-1:4 IAL	2.37	4.33	90.4	1.02
84CYM19-1:4 IAL	2.14	3.87	87.9	1.39
84CYM19-1:4 IAL	2.45	5.37	87.4	1.54
84CYM19-1:4 IAL	3.06	5.97	90.7	1.48
84CYM19-1:4 IAL	4.27	7.46	89.7	1.14
84CYM19-1:4 IAL	3.56	6.34	89.1	1.30
84CYM19-1:4 IAL	3.18	5.62	91.5	1.20
84CYM19-1:4 IAL	5.41	8.22	91.5	1.08
84CYM19-1:4 IAL	4.86	7.89	92.2	1.08
84CYM19-1:4 IAL	3.06	5.65	89.8	1.05
84CYM19-1:4 IAL	4.72	8.95	92.0	0.88
84CYM19-1:4 IAL	5.00	7.97	90.4	1.10
84CYM19-1:4 IAL	3.35	5.41	88.8	0.91
84CYM19-1:4 IAL	3.46	5.28	89.1	0.83
84CYM19-1:4 IAL	4.73	8.21	90.2	0.87
84CYM19-1:4 IAL	3.70	5.58	91.3	0.99
84CYM19-1:4 IAL	3.49	2.75	91.4	1.05
84CYM19-1:4 IAL	1.80	2.13	90.7	1.08
84CYM19-1:4 IAL	3.03	2.61	92.7	0.89
84CYM19-1:4 IAL	3.39	5.28	91.1	0.94

84CYM19-1:4 IAL	1.71	2.74	90.3	0.96
84CYM19-1:4 IAL	3.94	7.30	91.8	0.88
84CYM19-1:4 IAL	4.92	6.06	91.4	0.98
84CYM19-1:4 IAL	3.48	5.54	90.2	0.77
84CYM19-1:4 IAL	4.75	7.35	90.0	0.93
84CYM19-1:4 IAL	7.05	11.1	92.6	0.78
84CYM19-1:4 IAL	4.24	7.53	92.7	0.87
84CYM19-1:4 IAL	1.78	3.86	89.1	1.22
84CYM19-1:4 IAL	3.19	4.97	89.3	1.31
84CYM19-1:4 IAL	4.82	7.67	89.1	1.19
84CYM19-1:4 IAL	3.62	6.12	88.3	1.18
84CYM19-1:4 IAL	5.40	8.79	91.5	1.46
84CYM19-1:4 IAL	3.66	3.27	89.0	1.93
84CYM19-1:4 IAL	2.74	3.26	90.7	1.55
84CYM19-1:4 IAL	4.11	3.87	91.4	1.68
84CYM19-1:4 IAL	4.14	6.02	89.4	1.52
84CYM19-1:4 IAL	3.71	5.83	89.1	1.66
84CYM19-1:4 IAL	3.61	5.95	89.1	1.48
84CYM19-1:4 IAL	3.72	6.86	89.6	1.75
84CYM19-1:4 IAL	3.41	5.82	89.8	1.07
84CYM19-1:4 IAL	3.44	5.83	86.9	1.59
84CYM19-1:4 IAL	4.45	7.07	88.9	1.17
84CYM19-1:4 IAL	4.27	6.65	88.8	0.90
84CYM19-1:4 IAL	4.08	6.55	89.0	1.06
84CYM19-1:4 IAL	4.39	6.19	88.3	0.85
84CYM19-1:4 IAL	4.23	7.19	88.1	0.80
84CYM19-1:4 IAL	4.57	6.96	88.0	0.85
84CYM19-1:4 IAL	3.71	6.41	87.2	0.87
84CYM19-1:4 IAL	3.96	6.92	89.6	0.84
84CYM19-1:4 IAL	4.71	4.23	89.3	0.76
84CYM19-1:4 IAL	2.83	2.39	90.4	0.86
84CYM19-1:4 IAL	2.51	2.77	89.7	1.04
84CYM19-1:4 IAL	2.42	2.82	90.6	0.96
84CYM19-1:4 IAL	3.46	3.38	90.2	1.00
84CYM19-1:4 IAL	3.00	3.59	90.7	0.95
84CYM19-1:4 IAL	4.85	6.68	92.0	0.83
84CYM19-1:4 IAL	8.03	7.23	90.9	0.68
84CYM19-1:4 IAL	2.66	4.71	89.4	1.09
84CYM19-1:4 IAL	3.48	4.68	87.7	1.23
84CYM19-1:4 IAL	2.48	3.81	88.3	1.42
84CYM19-1:4 IAL	4.16	5.94	88.5	0.87
84CYM19-1:4 IAL	2.47	3.54	92.7	1.41
84CYM19-1:4 IAL	2.55	3.05	93.3	1.17
84CYM19-1:4 IAL	4.38	4.82	94.4	1.36
84CYM19-1:4 IAL	1.62	2.47	90.7	0.97
84CYM19-1:4 IAL	2.15	2.52	89.9	0.96
84CYM19-1:4 IAL	1.86	2.53	89.3	0.90
84CYM19-1:4 IPG (BDY)	3.08	5.80	90.6	1.60
84CYM19-1:4 IPG (BDY)	3.67	5.75	91.2	1.72
84CYM19-1:4 IPG (BDY)	2.28	4.92	88.8	1.41
84CYM19-1:4 IPG (BDY)	3.94	4.91	88.9	1.79
84CYM19-1:4 IPG (BDY)	2.51	4.05	92.3	1.53
84CYM19-1:4 IPG (BDY)	1.84	2.63	89.9	1.77
84CYM19-1:4 IPG (BDY)	2.14	2.83	91.1	1.88
84CYM19-1:4 IPG (BDY)	7.48	4.07	92.3	0.78
84CYM19-1:4 IPG (BDY)	5.33	7.59	93.0	1.90
84CYM19-1:4 IPG (BDY)	3.68	6.49	89.4	1.55
84CYM19-1:4 IPG (BDY)	4.66	5.68	89.6	1.07
84CYM19-1:4 IPG (BDY)	3.04	5.13	91.3	1.55
84CYM19-1:4 IPG (BDY)	2.51	4.36	90.6	1.53
84CYM19-1:4 IPG (BDY)	2.54	3.78	89.7	1.79
84CYM19-1:4 IPG (BDY)	3.57	3.86	89.9	1.66
84CYM19-1:4 IPG (BDY)	2.27	2.75	91.3	1.60
84CYM19-1:4 IPG (BDY)	2.39	2.95	91.6	2.10
84CYM19-1:4 IPG (BDY)	2.28	2.75	90.1	1.77
84CYM19-1:4 IPG (BDY)	4.28	3.83	92.0	1.54
84CYM19-1:4 IPG (BDY)	4.43	4.42	92.5	1.51
84CYM19-1:4 IPG (BDY)	2.79	3.61	90.8	1.44
84CYM19-1:4 IPG (BDY)	3.68	3.26	89.2	1.57
84CYM19-1:4 IPG (BDY)	2.64	4.06	91.4	1.44
84CYM19-1:4 IPG (BDY)	3.27	4.03	93.4	1.65
84CYM19-1:4 IPG (BDY)	2.51	3.02	89.8	1.68
84CYM19-1:4 IPG (BDY)	2.81	3.05	90.0	1.64
84CYM19-1:4 IPG (BDY)	3.63	3.96	92.9	1.85
84CYM19-1:4 IPG (BDY)	4.30	4.87	91.0	1.68
84CYM19-1:4 IPG (BDY)	1.65	2.48	89.3	1.86
84CYM19-1:4 IPG (BDY)	3.85	5.42	90.1	1.90
84CYM19-1:4 IPG (BDY)	1.36	2.81	89.4	1.28
84CYM19-1:4 IPG (BDY)	2.55	3.79	90.3	1.62
84CYM19-1:4 IPG (BDY)	3.55	4.79	92.3	1.52

84CYM19-1:4 IPG (BDY)	2.35	3.67	91.2	1.69
84CYM19-1:4 IPG (BDY)	3.50	5.04	89.7	2.18
84CYM19-1:4 IPG (BDY)	3.18	4.86	89.5	1.84
84CYM19-1:4 IPG (BDY)	2.83	3.68	91.6	1.66
84CYM19-1:4 IPG (BDY)	3.22	4.94	90.1	1.73
84CYM19-1:4 IPG (BDY)	4.41	4.20	106.4	1.34
84CYM19-1:4 IPG (BDY)	2.93	3.73	104.1	1.65
84CYM19-1:4 IPG (BDY)	1.12	2.06	107.6	1.83
84CYM19-1:4 IPG (BDY)	3.19	4.66	92.6	1.51
84CYM19-1:4 IPG (BDY)	2.57	3.44	92.6	1.75

APPENDIX D

	oxide	SiO_2	Al_2O_3	Fe_2O_3	Na_2O	MgO	K_2O	CaO	PbO	CuO	P_2O_5	Cl
Corning B	Test wt%	62.5	4.78	0.33	16.1	1.03	0.99	8.97	0.44	2.58	0.81	0.16
	Reference content wt%	61.6	4.36	0.34	17.0	1.03	1	8.56	0.61	2.66	0.82	0.16
	Absolute error wt%	0.97	0.42	-0.01	-0.86	0.00	-0.01	0.41	-0.17	-0.08	-0.01	0.00
	Relative error %	1.58	9.72	-1.50	-5.08	-0.46	-0.66	4.78	-27.4	-2.97	-1.75	0.54
	RSD	1.14	5.57	6.56	1.50	4.24	2.71	3.10	7.48	6.75	2.43	17.8

	oxide	SiO_2	Al_2O_3	Fe_2O_3	Na_2O	MgO	K_2O	CaO	PbO	CuO	P_2O_5	Cl
Corning C	Test wt%	34.6	0.90	0.29	1.02	2.63	2.76	7.24	35.7	1.05	0.11	0.08
	Reference content wt%	34.9	0.87	0.34	1.07	2.76	2.84	5.07	36.7	1.13	0.14	0.20
	Absolute error wt%	-0.29	0.03	-0.05	-0.05	-0.13	-0.08	2.17	-1.02	-0.08	-0.03	-0.12
	Relative error %	-0.83	3.12	-13.4	-4.45	-4.59	-2.67	42.7	-2.78	-6.80	-24.4	-60.9
	RSD	0.73	4.42	8.31	2.82	2.78	2.39	5.42	2.14	9.62	2.74	13.8

	oxide	SiO_2	Al_2O_3	Fe_2O_3	Na_2O	MgO	K_2O	CaO	PbO	CuO	P_2O_5	Cl
Corning D	Test wt%	55.9	5.31	0.53	1.29	3.95	11.6	14.5	0.23	0.35	3.73	0.17
	Reference content Wt%	55.24	5.30	0.52	1.20	3.94	11.3	14.80	0.48	0.38	3.93	0.20
	Absolute error Wt%	0.63	0.01	0.01	0.09	0.01	0.27	-0.30	-0.25	-0.03	-0.20	-0.03
	Relative error %	1.14	0.22	1.84	7.52	0.35	2.42	-2.06	-51.6	-7.91	-4.97	-15.4
	RSD	1.41	5.43	7.63	2.69	2.68	2.27	4.60	6.94	9.71	5.32	19.3

	oxide	SiO_2	Al_2O_3	Fe	Na_2O	Mg	K	CaO	Pb	Cu	P	Cl	Sn
N610	Test wt%	70.7	1.83		13.6			11.3					
	Test ppm			476		551.3			359.8	473.5	544.2	349.7	414.6
	Reference content Wt%	72.3	2.11		13.8			11.8					
	Reference content ppm			457		465.3			413.3	430.3	342.5	470.0	396.3
	Absolute error wt%	-1.60	-0.28	19.0	-0.21	86.0		-0.54	-53.5	43.2	201.7	-120.3	18.3
	Relative error %	-2.21	-13.2	4.16	-1.51	18.5		-4.56	-13.0	10.0	58.9	-25.6	4.61
	RSD	0.67	10.2	5.64	2.95	5.67		3.40	21.6	9.39	9.07	44.9	3.16

References

Angelini, I., 2008. Faience production in northern and western Europe. In: Tite, M.S., Shortland, A.J. (Eds.), Production Technology of Faience and Related Early Vitreous Materials. Oxford School of Archaeology, Oxford, pp. 129–135.

Archaeology Institute of Shanxi Province, 2006. A brief excavation report on the tombs of the western Zhou located at Hengshui Town, Jiang county, Shanxi province. Wen Wu 8, 4–18 (in Chinese).

Brill, R.H., 1989. The chemical composition of a faience bead from China. J. Glass Stud. 31, 11–15.

Brill, R.H., Vocke, R.D., Wang, S., Zhang, F., 1991. A note on lead-isotope analyses of faience beads from China. J. Glass Stud. 33, 116–118.

Bouquillon, A., Kaczmarczyk, A., Vandiver, P.B., 2008. Faience production in the Near East and the Indus Valley. In: Tite, M.S., Shortland, A.J. (Eds.), Production Technology of Faience and Related Early Vitreous Materials. Oxford School of Archaeology, Oxford, pp. 93–109.

Fu, X., Gan, F., 2006. Chinese faience and frit. J. Chin. Ceram. Soc. 34 (4), 427–431 (in Chinese).

Gan, F., Hu, Y., Dong, J., Wang, L., Cheng, H., 2009. Analysis of Liaozhu and Liaoguan excavated from the Yinguo tomb in Pingdingshan, Henan province. J. Chin. Ceram. Soc. 37 (6), 1005–1016 (in Chinese).

Goriachev, A.A., 2004. The Bronze Age archaeological memorials in Semirechie. In: Linduff, K.M. (Ed.), Metallurgy in Ancient Eastern Eurasia from the Urals to the Yellow River. Edwin Mellen Press, Lewiston, pp. 109–138.

Gratuze, B., 2016. Glass characterization using laser ablation-inductively coupled Plasma-mass spectrometry methods. In: Dussubieux, L., Golitko, M., Gratuze, B. (Eds.), Recent Advances in Laser Ablation ICP-MS for Archaeology. Springer Verlag Berlin Heidelberg, pp. 179–185.

Gu, Z., Zhu, J., Xie, Y., Xiao, T., Yang, Y., Wang, C., 2014. Nondestructive analysis of faience beads from the Western Zhou dynasty, excavated from Peng State cemetery, Shanxi province, China. J. Anal. At. Spectrom. 29, 1438–1443.

Hao, W., Yang, Y., Zhu, J., Gu, Z., Xie, Y., Zhan, L., Wang, L., 2014. XANES investigation of Chinese faience excavated from Peng State Cemetery site in Western Zhou period (BC1046–BC771). J. Electron. Spectrosc. Relat. Phenom. 196, 133–135.

Hommel, P., Sax, M., 2014. Shifting materials: variability, homogeneity and change in the beaded ornaments of the Western Zhou. Antiquity 88, 1213–1228.

Institute of Archaeology, Chinese Academy of Social Sciences, 1991. Radiocarbon Dates in Chinese Archaeology (1965-1991). Wenwu Press, Beijing (in Chinese).

Institute of Archaeology, Chinese Academy of Social Sciences, 1999. Western Zhou Cemetery at Zhangjiapo. Encyclopedia of China Publishing House, Beijing (in Chinese).

Institute of Cultural Relics and Archaeology of Gansu Province, 2009. Zhou Tombs at Yujiawan Village, Chongxin County. Wenwu chubanshe, Beijing (in Chinese).

Joint Archaeological Team of Shanxi Provincial Institute of Archaeology, 2012. The Western Zhou cemetery at Dahekou in Yicheng county, Shanxi. Chin. Archaeol. 12 (1), 1–12.

Lei, Y., Xia, Y., 2015. Study on production techniques and provenance of faience beads excavated in China. J. Archaeol. Sci. 52, 32–42.

Li, B., 2002. On excavation and study of the Jin cemetery. In: Museum, Shanghai (Ed.), Proceedings of the Symposium on Bronzes from the Cemetery of Marquises of Jin. Shanghai Fine Arts Publisher, Shanghai, pp. 29–40 (in Chinese).

Li, S., 2002. The interaction between Northwest China and Central Asia during the second millennium BC: an archaeological perspective. In: Boyle, K., Renfrew, C., Levine, M. (Eds.), Ancient Interactions: East and West in Eurasia. McDonald Institute for Archaeological Research, Cambridge, pp. 171–182.

Liu, N., Yang, Y., Wang, Y., Hu, W., Jiang, X., Ren, M., Yang, M., Wang, C., 2017. Nondestructive characterization of ancient faience beads unearthed from Ya'er

cemetery in Xinjiang, Early Iron Age China. Ceram. Int. 43, 10460–10467.
Lu, L., Hu, Z., 1998. The Cemetery of the Yu Polity at Baoji, vol. 2 Wenwu Press, Beijing (in Chinese).
Luo, X., 1995. The Beilu Zhou Cemetery. Xibei University Press, Xi'an (in Chinese).
Ma, Q., Zhang, Z., Xia, Y., 2009. The research review of Chinese Blue and Chinese Purple. In: In: Chinese Academy of Cultural Heritage (Ed.), Scientific and Technological Research on Cultural Heritage, vol. 6. Kexue chubanshe, Beijing, pp. 64–76 (in Chinese).
Miyake, Toshihiko, 2005. A preliminary study on Kayue bronzes. Kaogu (Archaeology) 5, 73–88 (in Chinese).
Qinghai Provincial Institute of Cultural Relics and Archaeology, Department of History and Archaeology of Xibei University & Institute of Hualong County Culture Administration, 1996. Preliminary excavation report on Banzhuwa burials of Kayue culture at Hualong county of Qinghai province. Kaogu (Archaeology) 8, 27–44 (in Chinese).
Rawson, J., 2013. Ordering the exotic: ritual practices in the late Western and early Eastern Zhou. Artibus Asiae 73, 1–76.
Rehren, Th, 2008. A review of factors affecting the composition of early Egyptian glasses and faience: alkali and alkali earth oxides. J. Archaeol. Sci. 35, 1345–1354.
Ren, X. (Ed.), 2013. Reappearance of Civilization: Important Archaeological Discoveries in the Course of Construction Work. Wenwu Press (Cultural Relics), Beijing (in Chinese).
Shandong Provincial Institute of Cultural Relics and Archaeology, 1996. Excavation of tomb 6 at Liutaizi. Jiyang, Shandong, Wenwu (Cultural Relics) 12, 4–25 (in Chinese).
Shandong Provincial Institute of Cultural Relics and Archaeology, Cultural Heritage Bureau of Jinan city, Cultural Bureau of Dezhou city, Cultural Bureau of Jiyang County (Eds.), 2010. Studies on the Jades Uncovered from Liutaizi at Jiyang, Shandong. Zhongzhi Fine Arts Publisher, Taipei (in Chinese).
Shortland, A., Shishlina, N., Egorkov, A., 2007. Origin and production of faience beads in the north Caucasus and the northwest Caspian Sea region in the Bronze Age. In: Lyonnet, B. (Ed.), Les Cultures du Caucase. CNRS Editions, Paris, pp. 269–283.
Shui, T., 2001. Papers on the Bronze Age Archaeology of Northwest China. Kexue Press, Beijing (in Chinese).
The School of Archaeology and Museology Beijing University, The Institute of Archaeology of Shanxi Province, 2001. The 6th season of excavation of the graveyard of Marquis of Jin at the Tianma-Qucun site. WenWu 8, 4–21 (in Chinese).
Tite, M.S., Shortland, A., Maniatis, Y., Kavoussanaki, D., Harris, S.A., 2006. The composition of the soda-rich and mixed alkali plant ashes used in the production of glass. J. Archaeol. Sci. 33, 1284–1292.
Vandiver, P.B., 2008. Raw materials and fabrication methods used in the production of faience. In: Tite, M.S., Shortland, A.J. (Eds.), Production Technology of Faience and Related Early Vitreous Materials. Oxford School of Archaeology, Oxford, pp. 37–55.
Wang, S., 1991. Some glasses from Zhou dynasty tombs in Fufeng County and Baoji, Shaanxi. In: Brill, R.H., Martin, J.H. (Eds.), Scientific Research in Early Chinese Glass: Proceedings of the Archaeometry of Glass Sessions of the 1984 International Symposium on Glass. The Corning Museum of Glass, Corning, pp. 151–156.
Xinjiang Institute of Cultural Relics and Archaeology, 2013. Saensayi Cemetery in Xinjiang. Wenwu chubanshe, Beijing (in Chinese).
Xu, X., 1988. On typology of Kayue culture. Qinghai Wenwu (Qinghai Cultural Relics) 1, 35–44 (in Chinese).
Xu, X., 1989. On typology of Kayue culture. Qinghai Wenwu (Qinghai Cultural Relics) 2, 38–44 (in Chinese).
Yang, J.H., Shao, H.Q., Pan, L., 2016. The Metal Road of the Eastern Eurasian Steppe. Shanghai Guji Press, Shanghai (in Chinese).
Yu, W., 1985. Collection of Archaeological Treatises on the Pre-Qin and Han Dynasties. Wenwu Press, Beijing (in Chinese).
Zhang, F., Cheng, Z., Zhang, Z., 1983. An investigation of ancient Chinese "Liuli". J. Chin. Ceram. Soc. 11 (1), 67–76 (in Chinese).
Zhang, Z., Ma, Q., 2009. Faience beads of the Western Zhou dynasty excavated in Gansu province, China: a technical study. In: Gan, F., Brill, R.H., Tian, S. (Eds.), Ancient Glass Research along the Silk Road. World Scientific, Singapore, pp. 275–289.